



National Library
of Canada

Bibliothèque nationale
du Canada

Canadian Theses Service

Service des thèses canadiennes

Ottawa, Canada
K1A 0N4

NOTICE

The quality of this microform is heavily dependent upon the quality of the original thesis submitted for microfilming. Every effort has been made to ensure the highest quality of reproduction possible.

If pages are missing, contact the university which granted the degree.

Some pages may have indistinct print especially if the original pages were typed with a poor typewriter ribbon or if the university sent us an inferior photocopy.

Previously copyrighted materials (journal articles, published tests, etc.) are not filmed.

Reproduction in full or in part of this microform is governed by the Canadian Copyright Act, R.S.C. 1970, c. C-30.

AVIS

La qualité de cette microforme dépend grandement de la qualité de la thèse soumise au microfilmage. Nous avons tout fait pour assurer une qualité supérieure de reproduction.

S'il manque des pages, veuillez communiquer avec l'université qui a conféré le grade.

La qualité d'impression de certaines pages peut laisser à désirer, surtout si les pages originales ont été dactylographiées à l'aide d'un ruban usé ou si l'université nous a fait parvenir une photocopie de qualité inférieure.

Les documents qui font déjà l'objet d'un droit d'auteur (articles de revue, tests publiés, etc.) ne sont pas microfilmés.

La reproduction, même partielle, de cette microforme est soumise à la Loi canadienne sur le droit d'auteur, SRC 1970, c. C-30.

Thermal Dissociation of Carbon Monoxide from Heme Peroxidases

Mariam Monshipouri

A Thesis

in

The Department

of

Chemistry

Presented in Partial Fulfillment of the Requirements
for the Degree of Master of Science at
Concordia University
Montréal, Québec, Canada

September 1988

Permission has been granted to the National Library of Canada to microfilm this thesis and to lend or sell copies of the film.

The author (copyright owner) has reserved other publication rights, and neither the thesis nor extensive extracts from it may be printed or otherwise reproduced without his/her written permission.

L'autorisation a été accordée à la Bibliothèque nationale du Canada de microfilmer cette thèse et de prêter ou de vendre des exemplaires du film.

L'auteur (titulaire du droit d'auteur) se réserve les autres droits de publication; ni la thèse ni de longs extraits de celle-ci ne doivent être imprimés ou autrement reproduits sans son autorisation écrite.

ISBN 0-315-44842-3

ABSTRACT

Thermal Dissociation of Carbon Monoxide from Heme Peroxidases.

Mariam Monshipouri

Thermal dissociation rates of the carbon monoxide (CO) adduct of ferrocyanochrome c peroxidase (CCP:CO) were measured in 0.01 M phosphate buffer, pH 7.0 at $18 \pm 0.5^\circ\text{C}$. The dissociation rate was measured by trapping the reduced enzyme with NO or H_2O_2 , to liberate the NO adduct of ferrocyanochrome c peroxidase and ferricytochrome c peroxidase (Fe^{IV}), respectively. Thermal dissociation rates of the CO adduct of Ferrihorseradish peroxidase were also measured, using NO as a trap.

At 1 atm CO, the CCP:CO dissociation process was biphasic with rate constants of $3.5 \pm 0.4 \times 10^{-3} \text{ s}^{-1}$ and $7.8 \pm 1.0 \times 10^{-2} \text{ s}^{-1}$. At 0.1 atm CO, only the slow rate was observed with $k = 2.9 \pm 0.6 \times 10^{-3} \text{ s}^{-1}$. The thermal dissociation rate of CCP:CO at pH 8.0 was also monophasic and $k = 3.7 \pm 0.3 \times 10^{-3} \text{ s}^{-1}$. These findings are compatible with resonance Raman and infrared data which reported alternative CO binding modes to ferrocyanochrome c peroxidase (Smulevich et al., Biochemistry, 1986, 25, 4426). Fresh CCP:CO dissociation in 0.1M phosphate buffer pH=8 was ~ 3 fold higher than that for moderately aged CCP:CO. This contrasts with inhibition of acidic-alkaline transition of Fresh CCP:CO in 0.1M phosphate buffer, reported by the latter researchers.

At 1 atm CO, the reaction of horse heart ferricytochrome c with CCP:CO was biphasic with k 's $= 1.3 \pm 0.5 \times 10^{-2} \text{ s}^{-1}$ and $2.0 \pm 0.2 \times 10^{-3} \text{ s}^{-1}$. At 0.1 atm CO, the reaction was monophasic with a rate constant of $1.5 \pm 0.4 \times 10^{-3} \text{ s}^{-1}$. The reaction of yeast ferri-

iv.

cytochrome c with CCP:CO was also biphasic at 1 atm CO, with $k's = 3.0 \pm 0.8 \times 10^{-2} s^{-1}$ and $3.0 \pm 0.7 \times 10^{-3} s^{-1}$. At 0.1 atm CO, the reaction was monophasic with a rate constant of $1.0 \pm 0.1 \times 10^{-2} s^{-1}$.

The activation parameters ($\Delta H^* = 6.4 \text{ Kcal mol}^{-1}$, $\Delta S^* = -47 \text{ e.u.}$) for the reactions of horse heart cytochrome c with CCP:CO indicate that cytochrome c may directly oxidize CCP:CO. Since the proteins form an electrostatically-stabilized complex at low ionic strength, we assume that electron transfer occurs within the C:CCP:CO complex.

ACKNOWLEDGEMENTS

I would like to thank the members of my research committee for their advice. Parts of this research was carried out through the use of Cary 2290 spectrophotometer that Dr. Jack Kornblatt made available to us, and I would like to thank him for this kindness. Last but not least, I owe gratitude to my fellow students in Room H-1149-1, particularly Eddy Cheung, for their support and friendship.

ABBREVIATIONS:

CCP	=	cytochrome c peroxidase
HRP	=	horseradish peroxidase
CCP:CO	=	carbon monoxide adduct of ferrocyclochrome c peroxidase
CCP:NO	=	nitric oxide adduct of ferrocyclochrome c peroxidase
HRP:CO	=	carbon monoxide adduct of ferrohorserradish peroxidase
HRP:NO	=	nitric oxide adduct of ferrohorserradish peroxidase
Mb	=	myoglobin
Hb	=	hemoglobin
CCP ^{IV}	=	ferrylcytochrome c peroxidase.
k ^I	=	slow dissociation rate constant for CCP:CO and HRP:CO at pH 7.0
k ^{I, I}	=	fast dissociation rate constant for CCP:CO and HRP:CO at pH 7.0
k ^{I, I'}	=	dissociation rate constant for CCP:CO at alkaline pH
ΔA_t^I	=	absorbance change due to slow portion of CCP:CO and HRP:CO thermal dissociation, at any given time.
$\Delta A_t^{I, I'}$	=	absorbance change due to fast portion of CCP:CO and HRP:CO thermal dissociation, at any given time.
ΔA_t	=	total absorbance change for CCP:CO and HRP:CO dissociation, at any given time.

ΔA_{∞}^i = maximum absorbance change due to slow portion of
CCP:CO and HRP:CO dissociation.

$I_0(\text{Rel})$ = relative intensity of incident beam.

c = cytochrome c

TABLE OF CONTENTS

	PAGE
ABSTRACT	iii
ACKNOWLEDGEMENTS	v
ABBREVIATIONS	vi
TABLE OF CONTENTS	viii
LIST OF FIGURES	xi
LIST OF TABLES	xiv
1. Introduction	1
2. Materials and Methods	
2.1. Materials	9
2.2. Methodology	9
2.3. Data Analysis	11
2.4. Investigation of Photo-Assisted Dissociation	14
3. Thermal Dissociation of CO-Peroxidase Using NO and H ₂ O ₂ as Trapping Agents	
3.1. Introduction	18
3.2. Results	
3.2.1 Thermal Dissociation of CCP:CO at pH 7.0 Using NO as a Trap.	19
3.2.2 Thermal Dissociation of CCP:CO Using H ₂ O ₂ as a Trap.	26
3.2.3 Thermal Dissociation of HRP:CO at pH 7.0 Using NO as a Trap.	30
3.2.4 Thermal Dissociation of CCP:CO at pH 8.0 Using NO as a Trap.	30

3.2.5	Effect of Phosphate Concentration Upon Fresh CCP:CO Dissociation Rate Constant at pH 8.0, Using NO as a Trap.	36
3.3	Discussion	
3.3.1	Thermal Dissociation of CCP:CO and HRP:CO at pH 7.0.	40
3.3.2	Thermal Dissociation of CCP:CO at pH 8.0, Using NO as a Trap.	43
3.3.3	Effect of Phosphate Concentration on Thermal Dissociation of Fresh CCP:CO.	43
4.	Reactions of CCP:CO with Ferricytochrome c's from Yeast and Horse Heart.	
4.1	Introduction	45
4.2	Results	
4.2.1.1	Reaction of Horse Heart Ferricytochrome c with CCP:CO at 1 atm CO.	46
4.2.1.2	Temperature Dependence of the Reaction Rate of Horse Heart Ferricytochrome c with CCP:CO.	53
4.2.2	Reaction of Yeast Ferricytochrome c with CCP:CO at 1 atm CO.	58
4.2.3	Reaction of Horse Heart and Yeast Ferricytochrome c's with CCP:CO at 0.1 atm CO.	58
4.2.4	Thermal Dissociation of CCP:CO in the Presence of Yeast and Horse Heart Ferricytochrome c's Using NO as a Trap.	65
4.3	Discussion	
4.3.1	Reactions of Horse Heart and Yeast Ferricytochrome c's with CCP:CO, at 1 atm CO.	68
4.3.2	Reactions of Ferricytochrome c's with CCP:CO at 0.1 atm CO.	69

4.3.3	Thermal Dissociation of CCP:CO in the Presence of Reduced Yeast and Horse Heart Cytochrome c's Using NO as a Trap.	70
Conclusions		71
Suggestions for further experiments..		73
References.		75

LIST OF FIGURES

Figure	Title	Page
2.1	Semi-log plot of the data in Figure 3.2 for CCP:CO thermal dissociation	13
2.2	The percentage slow phase (% ΔA^1) of 3 μ M CCP:CO thermal dissociation versus $I_0(\text{Rel})$ at 1 and at 0.1 atm CO, in 0.01 M phosphate buffer pH 7.0, at $18 \pm 0.5^\circ\text{C}$.	16
2.3	The percentage slow phase ΔA^1 of 3 μ M HRP:CO thermal dissociation versus $I_0(\text{Rel})$ at 1 atm CO and 0.1 atm CO in 0.01 M phosphate buffer pH 7.0, at $18 \pm 0.5^\circ\text{C}$.	17
3.1	Soret absorption spectra of 2.5 μ M CCP:CO and CCP:NO in 0.01 M phosphate buffer pH 7.0, at room temperature.	20
3.2	Absorbance changes (ΔA_t) at 424 nm due to 3 μ M CCP:CO dissociation versus time in 0.01 M phosphate buffer pH 7.0, at $18 \pm 0.5^\circ\text{C}$, using NO as a trap, under 1 atm CO.	21
3.3	Semi-log plot of the data in Figure 3.2 for CCP:CO thermal dissociation.	22
3.4	Semi-log plot of the data in Figure 3.2 for CCP:CO dissociation over the first 28 s, which corresponds to 3 half lives for the fast phase ($k^{11} = 7.8 \times 10^{-2}\text{s}^{-1}$, Table III).	23
3.5	Absorbance changes at 424 nm due to 3 μ M CCP:CO dissociation versus time, in 0.01 M phosphate buffer pH 7.0, using H_2O_2 as a trapping agent under 1 atm CO.	28
3.6	Absorbance changes at 424 nm due to 3 μ M HRP:CO dissociation versus time, in 0.01 M phosphate buffer pH 7.0 at $18 \pm 0.5^\circ\text{C}$, using NO as a trapping agent, under 1 atm CO.	31
3.7	Semi-log plot of the data in Figure 3.6 for HRP:CO dissociation.	32
3.8	Semi-log plot of the data in Figure 3.6 for HRP:CO dissociation over the first 32 s which corresponds to ~ 3 half lives for the fast phase ($k^{11} = 7.2 \times 10^{-2}$, Table V).	33

Figure	Title	Page
3.9	Soret absorption spectra of 2.5 μM CCP:CO at different pH's in 0.01 M phosphate buffer at room temperature. The pH was adjusted by adding 0.2 N NaOH to the cuvette.	34
3.10	Absorbance change at 424 nm due to 3 μM CCP:CO thermal dissociation versus time. The reaction was carried out in 0.01 M phosphate buffer, pH 8.0, at $18 \pm 0.5^\circ\text{C}$, using NO as a trapping agent. The CO and NO pressures were both 1 atm.	35
3.11	Absorbance changes at 424 nm due to 2.5 μM fresh CCP:CO dissociation versus time, in 0.01 M phosphate buffer pH 8.0, at $18 \pm 0.5^\circ\text{C}$, using NO as trapping agent, under 1 atm CO. "Fresh" CCP:CO is defined in Section 3.2.5.	38
4.1	Soret absorption spectra of 2.5 μM CCP ^{III} and 2.5 μM CCP:CO in 0.01 M phosphate buffer, pH 7.0, at room temperature (Traces 1-4 were obtained after 2, 4, 6 and 8 s exposure of CCP ^{III} samples to UV light, respectively in order to form CCP:CO. The absorption of CCP:CO remained constant after 8 s and resembles trace 4).	48
4.2	Absorbance changes at 414 nm due to the reaction of 2.5 μM CCP:CO with ferricytochrome c in 0.01M phosphate buffer, pH 7.0, under 1 atm CO.	49
4.3	Semi-log plot of the data in Figure 4.2 for the reaction of horse heart ferricytochrome c and CCP:CO.	50
4.4	Semi-log plot of the data in Figure 4.2 for the reaction of horse heart ferricytochrome c and CCP:CO over the first 30 s. This corresponds to ~ 0.9 half lives of the fast phase ($k^{\text{II}} = 2.0 \times 10^{-2} \text{s}^{-1}$, Table VII).	51
4.5	Temperature dependence of the observed rate constants for the slow phase of horse heart ferricytochrome c and CCP:CO reaction in 0.01 M phosphate buffer pH 7.0, under 1 atm CO.	56

Figure	Title	Page
4.6	Absorbance changes at 414 nm due to the reaction of yeast ferricytochrome c with CCP:CO in 0.01 M phosphate buffer pH 7.0, at $18 \pm 0.5^\circ\text{C}$, under 1 atm CO.	59
4.7	Semi-log plot of the data in Figure 4.6 for the reaction of yeast ferricytochrome c and CCP:CO.	60
4.8	Semi-log plot of the data in Figure 4.6 for the reaction of yeast ferricytochrome c with CCP:CO over the first 30 s. This corresponds to ~ 1.3 half lives of the fast phase ($k^1 = 3.0 \times 10^{-2} \text{ s}^{-1}$, Table VII).	61
4.9	Absorbance changes at 414 nm due to the reaction of horse heart ferricytochrome c with CCP:CO versus time in 0.01 M phosphate buffer pH 7.0 at $18 \pm 0.5^\circ\text{C}$, under 0.1 atm CO.	62
4.10	Absorbance changes at 414 nm for the reaction of yeast ferricytochrome c with CCP:CO versus time in 0.01 M phosphate buffer pH 7.0, at $18 \pm 0.5^\circ\text{C}$ under 0.1 atm CO.	64
4.11	Absorbance changes at 414 nm due to CCP:CO thermal dissociation in presence of yeast ferrocycytochrome c versus time in 0.01 M phosphate buffer pH 7.0, at $18 \pm 0.5^\circ\text{C}$, under 0.05 atm CO, using NO as trapping agent.	66

LIST OF TABLES

Table	Title	Page
I	Kinetic Parameters and Vibrational Frequencies for CO Binding	5
II	Literature Assignments of the FeCO Vibrational Frequencies (cm^{-1}) for HRP:CO and CCP:CO	8
III	Thermal Dissociation Rate Constants for CCP:CO and HRP:CO in the presence of 6% transmittance ND filter, Using NO as a Trap	24
IV	Thermal Dissociation Rate Constants for CCP:CO and HRP:CO in the absence of ND filter, Using NO as a Trap	25
V	Thermal Dissociation Rate Constants for CCP:CO at pH 7.0, Using H_2O_2 as a Trap	29
VI	Thermal Dissociation Rate Constants for Fresh CCP:CO at pH 8.0, Using NO as a Trap	39
VII	Rate Constants for the Reaction of Ferricytochrome c's with CCP:CO at 1 atm CO	52
VIII	Observed Rate Constants (k_{f}^{H}) for the Fast Phase of the Reaction Between Horse heart Ferricytochrome c and CCP:CO versus Temperature at 1 atm CO	54
IX	Observed Rate Constants for the Slow Phase of the Reaction Between Horse Heart Ferricytochrome c and CCP:CO versus Temperature at 1 atm CO.	55
X	Activation Parameters for CO Dissociation from Mb:CO and HRP:CO.	57
XI	Rate Constants for the Reactions of Horse Heart and Yeast Ferricytochrome c's with CCP:CO at 0.1 atm CO	63
XII	Thermal Dissociation Rate Constants for CCP:CO in the Presence and Absence of Ferrocyanochrome c, Using NO as a Trap.	67

CHAPTER 1

INTRODUCTION:

Heme proteins accomplish diverse functions such as O_2 transport, electron transfer, H_2O_2 breakdown and several kinds of oxidation. These proteins employ iron porphyrin in their active sites. With the exception of the electron transfer proteins, the iron coordination number at the active site is five, so that the sixth position is open for ligand binding or catalytic activity.

Peroxidases are a group of hemoproteins which act as catalysts in the peroxidation of numerous substrates. Upon addition of strong reducing agents the resting ferriperoxidase changes to the ferro derivative, the spectrum of which is very similar to that of ferro Mb and ferro Hb. Ferropoxidase is unstable in the presence of O_2 reverting to the ferri form. With ligands such as CO, NO and CN^- , peroxidases form adducts similar to those of Hb and Mb.

The reactions of CO with hemes have long been of chemical and biochemical interest. This is largely because structural and chemical interpretations of bonding in transition metal carbonyls can be based upon CO stretching frequencies.

In the past decade, researchers forwarded evidence for various binding modes of CO to hemoproteins. Smith and coworkers (1983) reported that HRP:CO isoenzyme c exhibits two $\nu(CO)$ infrared bands at 1933.5 cm^{-1} and 1905 cm^{-1} . In D_2O the bands shift to 1932.5 cm^{-1} and 1902.5 cm^{-1} , which suggests the existence of a strong H-bond between oxygen of CO and a proton of a distal residue.

The spectrophotometric titration of a distal histidine revealed a

shift in pK_a from 7.25 to 8.25 upon combination of HRP with CO. This shift was again interpreted in terms of the presence of an H-bond between the bound CO and a distal base in HRP:CO (Hayashi et al., 1976). However, the X-ray structure of CO-bound hemoglobin revealed that the oxygen atom of CO is displaced from the heme normal (Baldwin, 1980), but no H-bonding is observed between bound CO and distal residues.

Structural studies of heme proteins have led to three distinct effects on reactivity of the heme towards ligands: the proximal base tension effect, the proximal imidazole deprotonation effect and the distal side steric effect (Dickerson and Geis, 1983; Takano (1977); Fermi (1975); Brozowski et al., 1984). The steric contact between the proximal imidazole and the porphyrin plane is known to control heme affinity in relaxed (R) and tense (T) states of Hb, towards O_2 . It is assumed that proximal imidazole deprotonation could also play a role in the affinity of the heme for O_2 or CO. It is proposed that the lowered affinity in T-state Hb is due to the H-bonding of proximal histidine, which is not present in the R-state.

Distal effects which influence ligand binding in hemoproteins can be of several types: steric, local polarity and hydrogen bonding. X-ray crystal structures of O_2 and CO bound iron II "picket fence" porphyrin complex, revealed that O_2 is bound in a bent fashion whereas CO is bound linearly (Jameson et al., 1980). The structure difference between the mode of binding of CO and O_2 was proposed as a mechanism for lowering the toxicity of CO. Collman et al. (1976), performed kinetic measurements on "picket fence" and pocket porphyrins and observed a 30

fold decrease in CO affinity upon crowding the porphyrin pocket, while the O₂ affinity remained unchanged. It was found that the association rates of both CO and O₂ decreased. Although the dissociation rate of O₂ decreased the corresponding rate for CO remained constant. Yu et al. (1983) prepared strapped hemes in which the length of the strap was systematically varied. They observed that as the strap was extended CO association rate increased (Table I). Hence these researchers predict that distal steric effects appear mainly in CO association rates. Traylor (1980) studied the CO and O₂ affinities of cyclophane and chelated hemes. His studies led him to suggest that the proximal side strains result in an equal change in association and dissociation rates whereas distal side steric effects appear entirely in the association rates. Hence according to Traylor in order to distinguish the distal from proximal side effects, upon ligand binding the knowledge of both dissociation and association rates are necessary.

The comparison of thermodynamic and kinetic parameters of model hemes with Hb revealed that O₂ and CO binding to Hb are not influenced by distal side steric effects and it is possibly the pocket polarity and not the configuration of Fe-CO bond which determines the relative O₂ and CO affinities (Chang et al., 1975; Gibel et al., 1978; Traylor et al., 1981).

Suslick et al. (1984) examined solvent influence on CO and O₂ binding affinities systematically. They observed that CO affinity decreased with solvent polarity, whereas O₂ affinity increased. However, the effect of solvent polarity on CO dissociation rate have not yet been reported.

Phillips et al. (1981) reported hydrogen bonding between bound dioxygen and the distal imidazole in Mb(O₂) and Hb(O₂)₄. Model compounds which have been used to study this interaction include, strapped porphyrin, (Mometeau and Lavalette, 1982), "basket handle" porphyrin and chelated porphyrin. Chang and coworkers when working with the latter porphyrin, revealed that on and off rates of O₂ but not CO are affected by the polar groups near the ligand binding site, (Young and Chang, 1985).

Recently, Spiro and coworkers reported alternative CO binding modes for HRP using resonance Raman and infrared spectroscopy (Evangelista-Kirkup et al., 1986). At acidic pH, HRP:CO, Form I, is observed with $\nu(\text{FeC}) = 490 \text{ cm}^{-1}$ and $\nu(\text{CO}) = 1932 \text{ cm}^{-1}$. The appearance of the FeCO bending mode in the Raman Spectrum has been suggested to be associated with FeCO bonds that are off axis relative to the heme normal (Baldwin, 1980). No $\delta(\text{FeCO})$ bending mode was observed with this species (Form I); hence the CO bending mode was assumed to be linear. Upon increasing the CO pressure at low pH, Form II of HRP:CO is observed with $\nu(\text{FeC}) = 437 \text{ cm}^{-1}$, $\nu(\text{CO}) = 1904 \text{ cm}^{-1}$ and $\delta(\text{FeCO}) = 587 \text{ cm}^{-1}$ (Table II). In the latter species CO is assumed to be tilted and H-bonded to a protonated distal histidine because of the FeCO bending mode observed. An equilibrium exists between Forms I and II which is shifted toward Form II upon increasing the CO concentration. This behaviour is interpreted to be due to the binding of a second CO molecule in the heme cavity which induces a conformational change involving the distal residues.

Table I : Kinetic Parameters and Vibrational Frequencies for CO Binding.

System	$k_{on}(CO)^f$ M ⁻¹ s ⁻¹	$k_{off}(CO)^f$ s ⁻¹	$P_{1/2}(CO)^f$ torr	$\gamma(CO)$ cm ⁻¹
<u>Mb</u>	1.5×10^7	0.005	0.02	1945 ^a
<u>Hb, R state</u>	4.6×10^6	0.009	0.0014	
<u>Hb, T state</u>	2.2×10^5	0.09	0.3	1951 ^b
<u>Picket Fence R state</u>	3.6×10^7	0.008	2.2×10^{-5}	1970 ^c
<u>Picket Fence T state</u>	1.4×10^6	0.14	8.9×10^{-3}	1969 ^c
<u>Strapped Heme</u>				
tight strap	8×10^3	0.04	0.5	
loose strap	9.1×10^4	0.04	0.05	
<u>capped porphyrin</u>	9.5×10^5	0.05	5.4×10^{-3}	1984 ^d
<u>chelated Heme</u>	1.1×10^7	0.015	1.0×10^{-3}	1957 ^e

This table was compiled from the following sources:

a: Caughey (1970), b: Antonioni and Brunori (1971), c: Collman et al. (1976),
d: Hoshimoto et al. (1982), e: Case et al. (1979) and Traylor et al. (1981),
f: Suellick and Reinert (1985).

Resonance Raman and infrared data of CCP:CO reported by Smulevich et al. (1986) also reveals two CO binding modes for CCP at low pH: Form I with $\nu(\text{FeC}) = 495 \text{ cm}^{-1}$, and no detectable $\delta(\text{FeCO})$, and Form II with

$\nu(\text{FeC}) = 530 \text{ cm}^{-1}$ and $\delta(\text{FeCO}) = 585 \text{ cm}^{-1}$ (Table II). Both forms have coincidental infrared bands at 1922 cm^{-1} . Form I is assumed to be linear, because no bending mode was detected, while Form II is assumed to be tilted and H-bonded to the distal histidine. For CCP:CO a single major CO infrared band occurs at $1920.4 \pm 0.5 \text{ cm}^{-1}$ in aqueous buffer which shifts by $2.0 \pm 0.5 \text{ cm}^{-1}$ in D_2O (Satterlee et al., 1984). Similar to HRP, the equilibrium between Forms I and II of CCP:CO are shifted towards the latter at elevated CO concentrations. At high pH, Form IV is converted into Form II', with $\nu(\text{FeC}) = 403 \text{ cm}^{-1}$, $\delta(\text{FeCO}) = 575 \text{ cm}^{-1}$ and $\nu(\text{CO}) = 1948 \text{ cm}^{-1}$. This form is assumed to be tilted due to the presence of an FeCO bending mode, but not H-bonded because the FeC stretching frequency is significantly less and the CO stretching frequency is considerably greater for Form II' compared to Form II.

To support the resonance Raman and infrared findings, kinetic evidence for different conformations of the peroxidase CO adducts was sought. A kinetic study should reveal whether the different CO conformers are in equilibrium or non-interconverting. In performing our kinetic measurements on the alternative CO adducts of peroxidases, we were restricted to studying only thermal dissociation rates since CO combination rates with the ferropoxidase cannot be measured following preincubation of the proteins with CO. In the present study, detailed measurements on CCP:CO and HRP:CO thermal dissociation using NO as

trapping agent are reported. Kinetic evidence for alternative CO binding modes to CCP and HRP is provided and the influence of the protein moiety on CO binding is discussed with reference to some model compounds.

Horse heart and yeast cytochrome c are known to bind to CCP at low ionic strength in solution (Mochan, 1970; Mochan and Nicholls, 1971; Gupta and Yonetani, 1973; Leonard and Yonetani, 1974; Erman and Vitello, 1980; Kang and Erman, 1982; Dowe and Vitello, 1984; Hoth and Erman, 1984; Kornblatt and English, 1986; Hazzard et al., 1987). The electron transfer rate between C^{III} and CCP^{II} was measured to be 0.23 s^{-1} and 1.7 s^{-1} for horse heart and yeast cytochrome c's, respectively (Cheung et al., 1986). The three dimensional structure of CCP has been elucidated at high resolution (Poulos et al., 1980; Finzel and Poulos, 1984; Poulos and Finzel, 1984). Poulos and Kraut, 1980 have proposed a model of CCP^{III} interacting with C^{II} . The model incorporates the charge interactions of the two proteins (Kang et al., 1978; Koppenol and Margoliash, 1982). Mochan and Nicholls, 1971 found that the rate of the reaction of H_2O_2 with CCP^{II} in the presence of cytochrome c is unaffected. Therefore, it is expected that CO can also bind with CCP^{II} in the presence of cytochrome c. In chapter 4, the reactions of horse heart and yeast C^{III} with CCP:CO are reported and the thermodynamic parameters of the reduction of horse C^{III} with CCP:CO are determined and the nature of the observed reactions are discussed. This study is to determine the effects of coordination number and spin state of the iron upon the intramolecular electron transfer rate in $C^{III}/CCP:CO$.

Table II: Literature Assignments of the FeCO Vibrational Frequencies
(cm^{-1}) for HRP:CO and CCP:CO

Protein	Form	$\nu(\text{CO})$	$\nu(\text{FeC})$	$\delta(\text{FeCO})$
HRP	I	1932	490 ^a	
HRP	II	1904	437 ^a	587
CCP	I	1922	495 ^b	
CCP	II	1922	530 ^b	585
CCP	II	1948	403 ^b	575

^a Evangelista-Kirkup et al., 1986;

^b Smulevich et al., 1986

CHAPTER 2

MATERIALS AND METHODS

2.1. Materials

CCP was isolated from bakers yeast (Fleishmans) according to the modified procedure of Nelson et al., 1977 by English et al., 1986. The crystals were found to have a purity index (A_{408}/A_{280}) of 1.2-1.4. HRP, (isoenzyme C) type VI, horse heart c (type VI), and yeast c (*Candida krusei*, type VII) were obtained from Sigma and were used without further purification. CO (c.p. grade), NO (c.p. grade) and argon (prepurified) were purchased from Union Carbide. CO and argon were passed through a chromous tower followed by a phosphate buffer (0.1M, pH 7.0) tower to obtain oxygen-free gases. NO was passed through a layer of KOH crystals to absorb unwanted higher oxides, and excess NO was oxidized to nitrate in a solution of NaOH and H_2O_2 .

2.2 Methodology:

Solutions of 2.5 - 3 μ M CCP or HRP were prepared in 0.01M or 0.1M phosphate buffer containing 0.008% wt/vol acetophenone and 2% wt/vol isopropyl alcohol. All samples were degassed under scrubbed argon for 1 hour. The degassed Fe^{III} enzyme samples were photoreduced to the Fe^{II} state in situ in the cuvette by the radicals which are generated when the acetophenone is exposed to the UV-light (Ward et al., 1982). HRP:CO and CCP:CO were generated according to the following procedure: the 1 atm CO samples were prepared by directly bubbling scrubbed CO into the enzyme solution for 15 min. To obtain CO pressures of 0.1 and 0.01 atm,

CO was introduced into the degassed solution by a gas syringe. All the samples were equilibrated for at least 5 min at the desired temperature, using a thermostatted bath. Using the tables of solubility of CO in solution (Weast, 1980) the CO concentration in 3 ml samples was estimated to be approximately 3 mM.

For NO displacement reactions, NO was bubbled into phosphate buffer to form a saturated NO solution, and NO concentration was estimated to be of approximately 6.6 mM using tables of solubility of NO in solution (Weast, 1980). An appropriate amount of this solution was then introduced into the cuvette by a gas syringe, so that the concentration of dissolved NO would always be twice that of CO in the buffer.

The dissociation reaction was measured 2-3 s after the injection of the appropriate amount of the trapping agent. The 2-3 s was allowed for mixing of the cuvette contents.

H₂O₂ solutions of known concentration were also prepared in phosphate buffer and were degassed for 1 hr before being injected into the cuvette. In this case also, the concentration of H₂O₂ was 2 times higher than that of CO in the buffer.

For cytochrome c reactions, ferricytochrome c solutions of known concentration were prepared in phosphate buffer and degassed for 45 min before being injected into the cuvette.

Absorbance changes were measured on a rapid scan HP9451A diode-array spectrophotometer (response time 0.1s). The sample in this instrument was exposed to a broad range of wavelengths which could cause photoassisted CO dissociation. Hence, CO thermal dissociation reactions were also measured by a Cary 2290 scanning spectrophotometer, to reduce

photoassisted CO dissociation a minimum. The results in both the cases were identical.

Each experiment was performed at least four times and the mean values of the rate constant, as well as standard deviations, are reported in the result sections of this thesis.

Extinction coefficients utilized throughout this work are as follows:

CCP^{III} : $\epsilon_{408} = 94 \text{ mM}^{-1} \text{ cm}^{-1}$ (Mathews and Wittenberg, 1979)

CCP:CO : $\epsilon_{424} = 150 \text{ mM}^{-1} \text{ cm}^{-1}$ (Yonetani and Ray, 1965)

CCP:NO : $\epsilon_{422} = 98 \text{ mM}^{-1} \text{ cm}^{-1}$ (pH 7.0) (Yonetani et al., 1972)

CCP:NO : $\epsilon_{422} = 68 \text{ mM}^{-1} \text{ cm}^{-1}$ (pH 8.0) (This work)

CCP^{IV} : $\epsilon_{428} = 100 \text{ mM}^{-1} \text{ cm}^{-1}$ (Mathews and Wittenberg, 1979)

HRP^{III} : $\epsilon_{404} = 100 \text{ mM}^{-1} \text{ cm}^{-1}$ (Ohlsson and Paul, 1976)

HRP:CO : $\epsilon_{422} = 137 \text{ mM}^{-1} \text{ cm}^{-1}$ (Kertesz et al., 1965)

HRP:NO : $\epsilon_{422} = 106 \text{ mM}^{-1} \text{ cm}^{-1}$ (Yonetani et al., 1972)

CCP^{III} and CCP^{IV} isosbestic at 413 nm: $89 \text{ mM}^{-1} \text{ cm}^{-1}$

CCP^{III} and CCP:CO isosbestic at 414 nm: $124 \text{ mM}^{-1} \text{ cm}^{-1}$

2.3 Data Analysis

In order to analyse the data and determine the order of the reaction a computer program was used to execute the Guggenheim, Kozdy-Swinbourne and Natural logarithm routines (Ng Ching Hing, 1985).

The data was subjected to Guggenheim and the Kozdy-Swinbourne methods to find the absorbance at infinity, then the natural logarithm method was applied to the same data, in order to determine the rate constant. The absorbance decay or growth versus time were both treated

with the same program, as described below:

The computer program extrapolated the absorbance versus time data to where the absorbance no longer changed with time. The asymptote to this curve was intercepted with the absorbance coordinate to yield A_{∞} (base line). The base line, A_{∞} , was subtracted from the absorbance at any time and the log was taken from this value to yield $\ln(\Delta A_t)$. The plot of $\ln(\Delta A_t)$ versus time was then subjected to a natural log first order routine in order to determine the rate constant. However, it was found that the data points in some cases could not fit satisfactorily, with a single straight line. For example, CCP:CO thermal dissociation using NO as trapping agent shown in Chapter 3 (Figure 3.2) could not be analysed using a single first order fit. The following three steps were taken in order to analyse this type of data, which was found frequently during the course of this study.

1. In Figure 2.1, shown below where all the data points were treated by a single first order fit the beginning portion of the data points curve off and result in unsatisfactory correlation coefficients. From this plot, the time period due to fast portion of CCP:CO thermal dissociation was estimated to be 28 s.

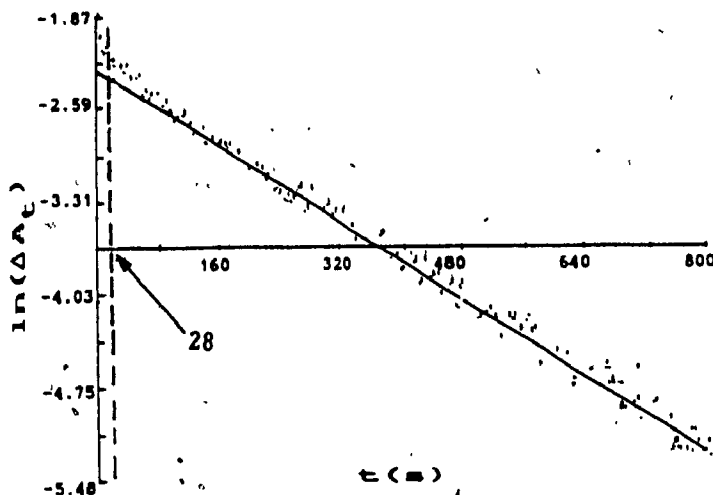


Figure 2.1 Semi-log plot of the data in Figure 3.2 for CCP:CO dissociation.

2. The slow portion of absorbance versus time data (28 - 800 s) was extrapolated, independently to where the absorbance no longer changed with time. The intercept of the asymptote to this curve with the absorbance coordinate results A_{∞}^I , which is the base line due to slow portion of CCP:CO thermal dissociation. A_{∞}^I was then subtracted from the absorbance at any time within 28 - 800 s to result ΔA_t^I . The plot of $\ln(\Delta A_t^I)$ versus time was then subjected to first order fit, the slope of which results k^I , which is the slow thermal dissociation rate constant.

3. The data for the first 28 s was independently extrapolated to where the absorbance no longer changed with time. The asymptote to this curve was intercepted with the absorbance coordinate to result A_{∞}^{II} (the

base line for the fast portion of CCP:CO thermal dissociation). A_{∞}^{11} was subtracted from absorbance versus time data at any time within 0-28 s to result ΔA^{11} . The plot of $\ln(\Delta A^{11})$ versus time was then subjected to a new first order fit to result k^{11} which is the rate constant for the fast portion of the CCP:CO thermal dissociation reaction.

In the cases where the absorbance versus time data could be best fit by two independent first order fits, the CCP:CO thermal dissociation reaction was assumed to be biphasic. This was because the resolution of the data into two linear plots correspond to the biphasic kinetics described by Swinbourne (1971) where two parallel first order reactions produce the same product. For the cases where a single straight line was sufficient to fit all the data points satisfactorily, the CCP:CO thermal dissociation reaction was assumed to be monophasic.

The correlation coefficients obtained during this study were within the range of 0.989-0.995.

2.4 Investigation of Photoassisted Dissociation

Heme-CO complexes are known to be extremely light sensitive (Brunori et al., 1972; Bonaventura et al., 1973). Consequently it is possible that some error is introduced in the magnitude of the thermal dissociation rate constants due to photolysis of the Heme-CO complexes. Also, the fast component observed for CCP:CO and HRP:CO dissociation at 1 atm may be due to photolysis rather than thermal dissociation.

In order to clear these problems, the percentage slow phase $\% \Delta A_{\infty}^{11}$, obtained according to Section 2.3, is plotted versus $I_0(\text{Rel})$ which is

the relative intensity of the incident beam, controlled by using neutral density (ND) filters, for CCP:CO (Figure 2.2) and HRP:CO (Figure 2.3). As can be seen in Figure 2.2, the slow portion of absorbance change due to CCP:CO thermal dissociation (ΔA_{∞}^I) at 1 atm CO increases with decreasing $I_0(\text{Rel})$, but remains constant and does not reach 100% even when $I_0(\text{Rel})$ is $\leq 12\%$, (i.e. there is always a fast portion present). At such low intensity, it is reasonable to assume that photoassisted dissociation is negligible. This suggests that CCP:CO thermal dissociation is definitely biphasic and the fast component of absorbance change due to CCP:CO dissociation is not due to photolysis. At 0.1 atm CO, (Figure 2.2), ΔA_{∞}^I increases with decreasing $I_0(\text{Rel})$ and reaches 100% when $I_0(\text{Rel}) \leq 15\%$. At these low intensities of the incident beam, photoassisted dissociation is most probably avoided, since upon decreasing the light intensity neither the absorbance nor the magnitude of the dissociation rate constant of CCP:CO dissociation is changed. Also, there is no fast component observed due to CCP:CO dissociation at 0.1 atm CO. Figure 2.3 shows $\% \Delta A_{\infty}^I$ versus $I_0(\text{Rel})$ for HRP:CO. As can be seen, HRP:CO almost mirrors the behaviour of CCP:CO at 1 and 0.1 atm CO.

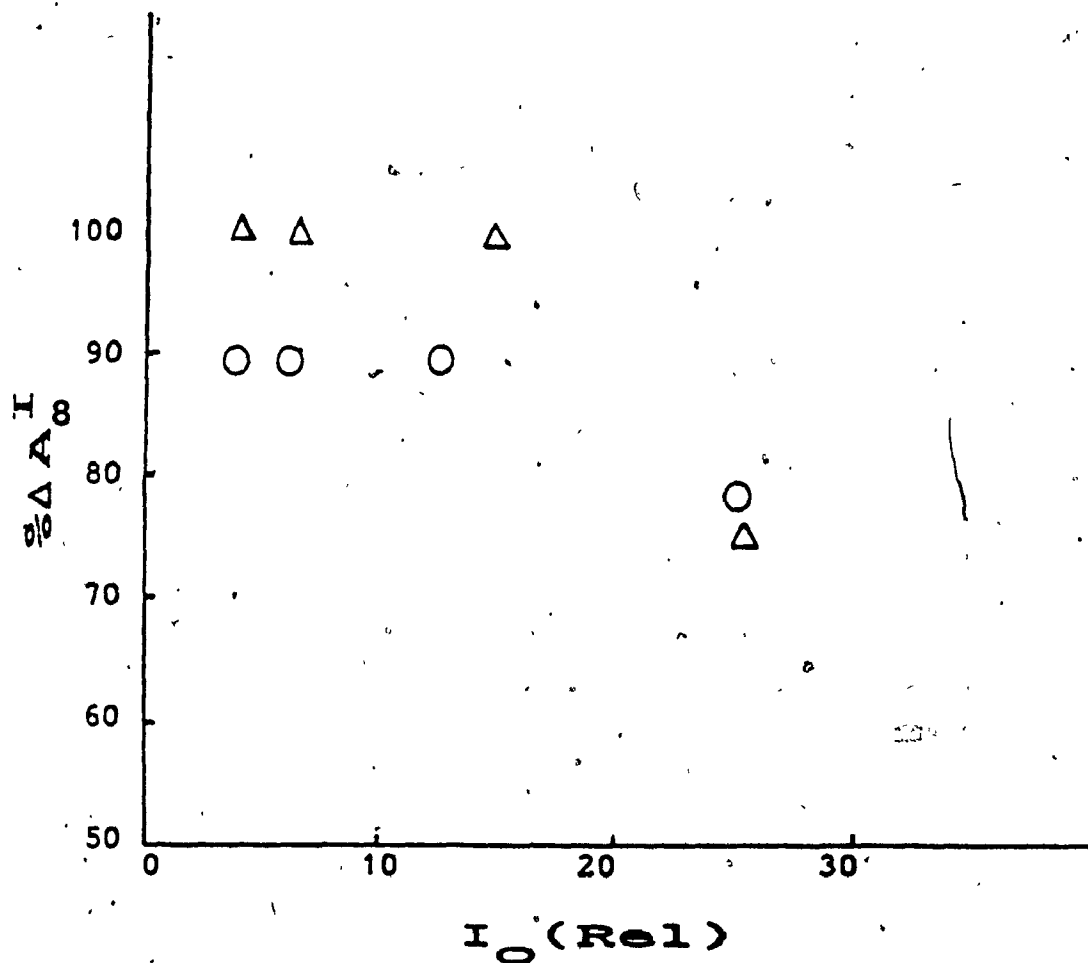


Figure 2.2 The percentage slow phase ($\% \Delta A_8^I$) of 3 μ M CCP:CO thermal dissociation versus I_0 (Rel) at 1 atm CO (O) and at 0.1 atm CO (Δ), in 0.01 M phosphate buffer pH 7.0, at $18 \pm 0.5^\circ\text{C}$.

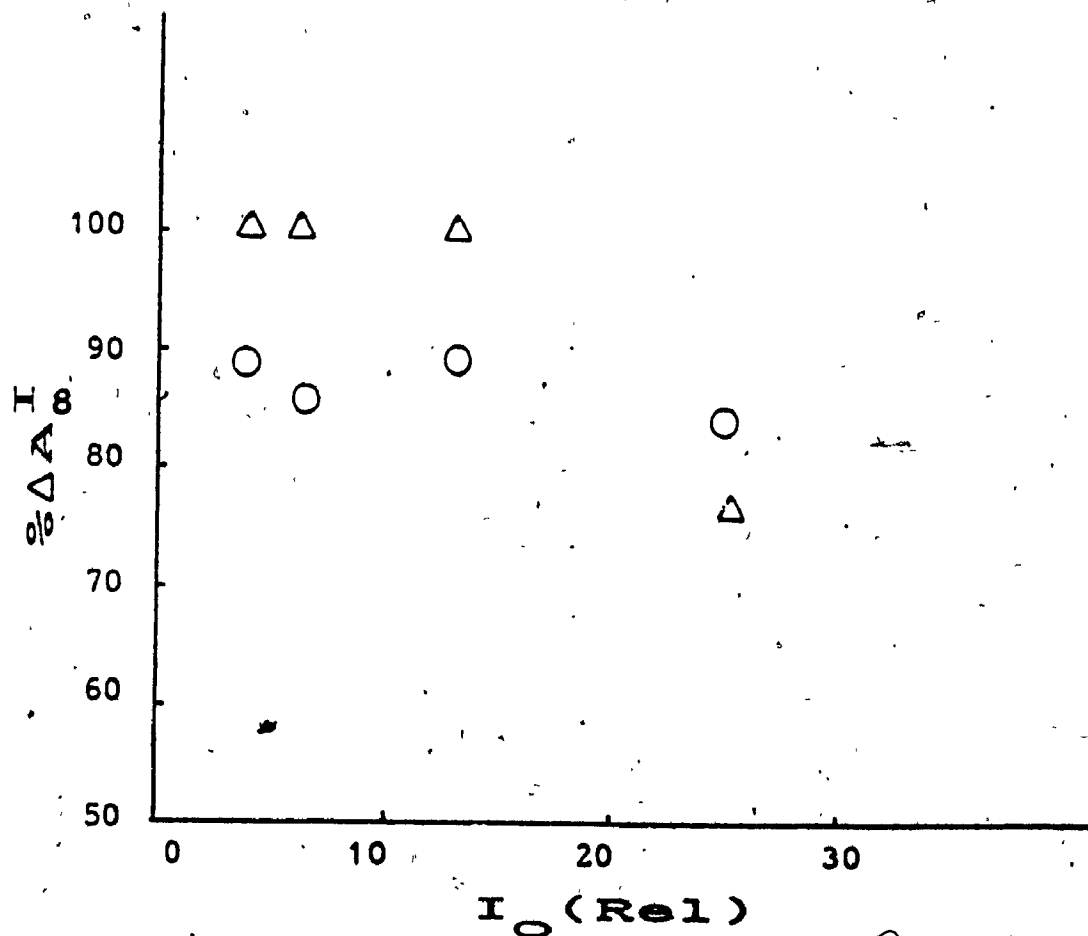


Figure 2.3 The percentage slow phase ($\% \Delta A^I$) of 3-M HRP:CO thermal dissociation versus $I_0(\text{Rel})$ at 1 atm CO (o) and at 0.1 atm CO (Δ) in 0.01 M phosphate buffer pH 7.0, at $18 \pm 0.5^\circ\text{C}$.

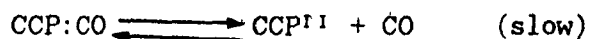
CHAPTER 3

THERMAL DISSOCIATION OF CO-PEROXIDASE USING NO AND H₂O₂ AS

TRAPPING AGENTS

3.1 Introduction

The CO dissociation from CCP:CO is predicted to occur according to the following Scheme:



This procedure is based on the assumption that CO dissociation is slow and rate-limiting, and the trapping ligand reacts with the non ligated derivative rapidly. In the following sections, NO and H₂O₂ were used as traps. The NO association rate constant with ferro-HRP was estimated to be $2.2 \times 10^5 \text{ M}^{-1}\text{s}^{-1}$ (Mims et al., 1983) and H₂O₂ reacts with peroxidases at the rate of 10^7 to $10^8 \text{ M}^{-1}\text{s}^{-1}$ (Chance, 1952; George, 1953; Yonetani, 1976; Loo and Erman, 1975). The rate constant for CO combination with reduced HRP was obtained using stopped flow experiments. At pH 7.0, in 0.1 M phosphate buffer the CO combination rate was $2.3 \times 10^3 \text{ M}^{-1}\text{s}^{-1}$ (Kertesz et al., 1965). The dissociation of CO from HRP:CO has been measured by cyanide (CN⁻) displacement. The magnitude of the CO dissociation rate constant was 0.025 s^{-1} at pH 9.1 (Phelps et al., 1971). Cyanide (CN⁻) binding occurs in one step at pH 9.1 but is more complicated at pH 6.0. Therefore, due to pH limitation and complexity of binding, cyanide was not used for our experiments. The HRP:CO thermal dissociation rate constant as reported by Wittenberg et al.,

1967 and Coletta et al., 1986, at pH 7.0 is $7.2 \times 10^{-5} \text{ s}^{-1}$ and $1.1 \times 10^{-4} \text{ s}^{-1}$, respectively. This rate is much slower than the dissociation rates cited for Mb:CO and Hb:CO $5 \times 10^{-3} \text{ s}^{-1}$ and $9 \times 10^{-3} \text{ s}^{-1}$ respectively, (Antonioni and Brunori, 1971; Sawicki and Gibson, 1977). Based on the available data it is reasonable to assume that the ferropoxidase:CO dissociation rates are a lot slower than either H_2O_2 or NO ferropoxidase association rates, and the latter ligands are suitable as trapping agents in the above Scheme.

3.2 Results

3.2.1 Thermal Dissociation of CCP:CO at pH 7.0, using NO as a Trap.

Figure 3.1 shows the Soret absorption spectra of CCP:CO and CCP:NO. Hence, upon occurrence of the following reaction a large absorbance decay was expected at 424 nm:

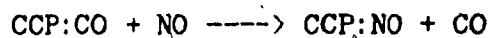


Figure 3.2 demonstrates a typical NO displacement reaction at 1-atm CO in 0.01 M phosphate buffer pH 7.0, using a 6% transmittance ND filter. The final product was determined spectrophotometrically. A characteristic peak at 422 nm revealed the presence of CCP:NO and its concentration was found to be close to the expected value of 2.5-3 μM depending on the concentration of CCP:CO originally present. The semi-log plots of absorbance change versus time are shown in Figures 3.3 and 3.4. The data were analyzed according to the procedures given in Section 2.3. The results indicate biphasic kinetics and the rate constants for the slow and fast phase of the CO dissociation reaction

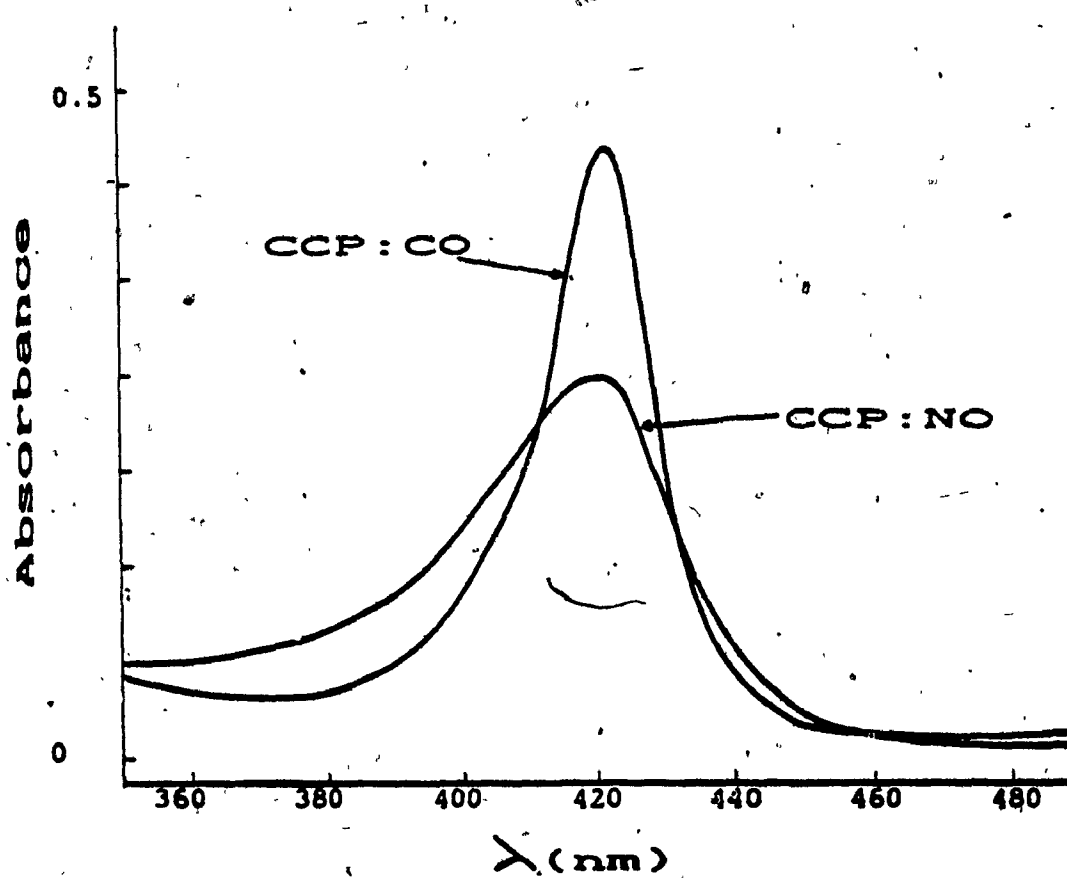


Figure 3.1 Soret absorption spectra of 2.5 μ M CCP:CO and CCP:NO in 0.01 M phosphate buffer pH 7.0, at room temperature.

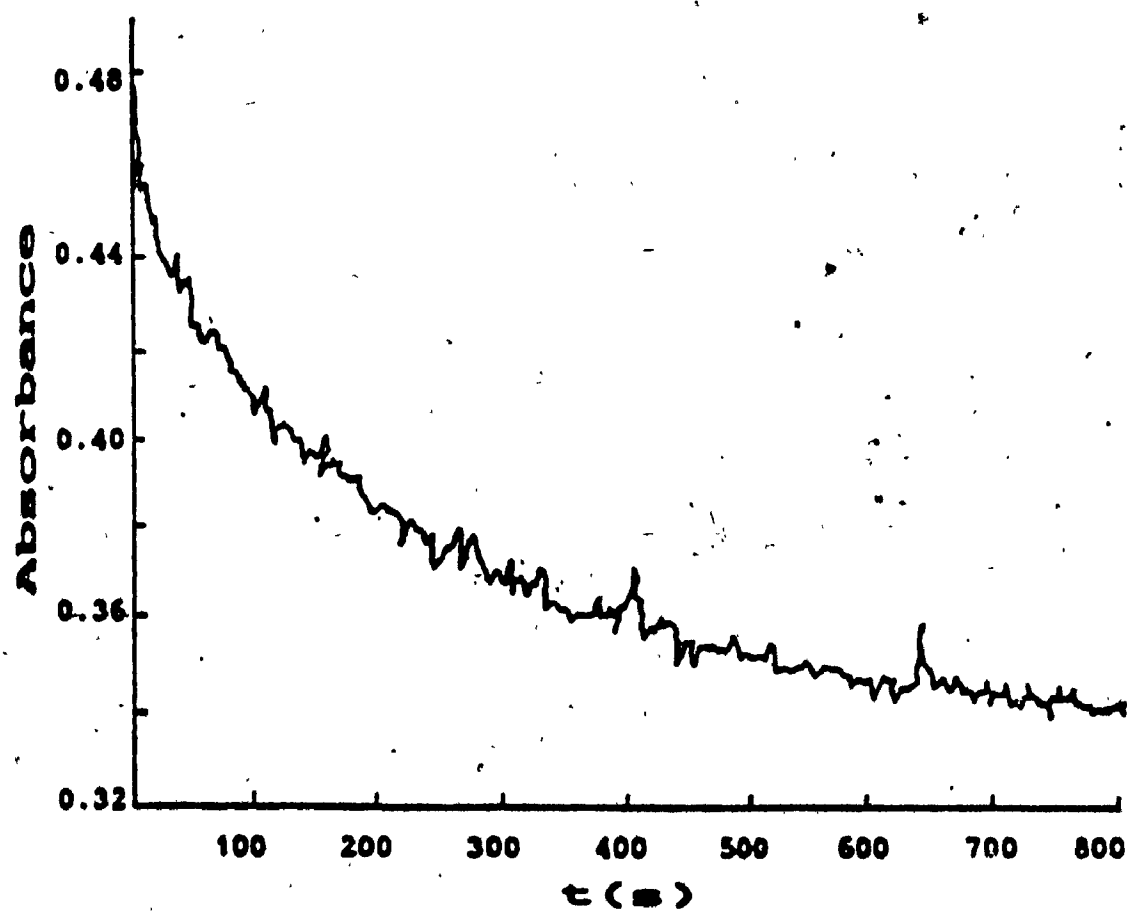


Figure 3.2 Absorbance change at 424 nm due to $3 \mu\text{M}$ CCP:CO dissociation versus time in 0.01 M phosphate buffer pH 7.0, at $18 \pm 0.5^\circ\text{C}$, using NO as a Trap, under 1 atm CO.

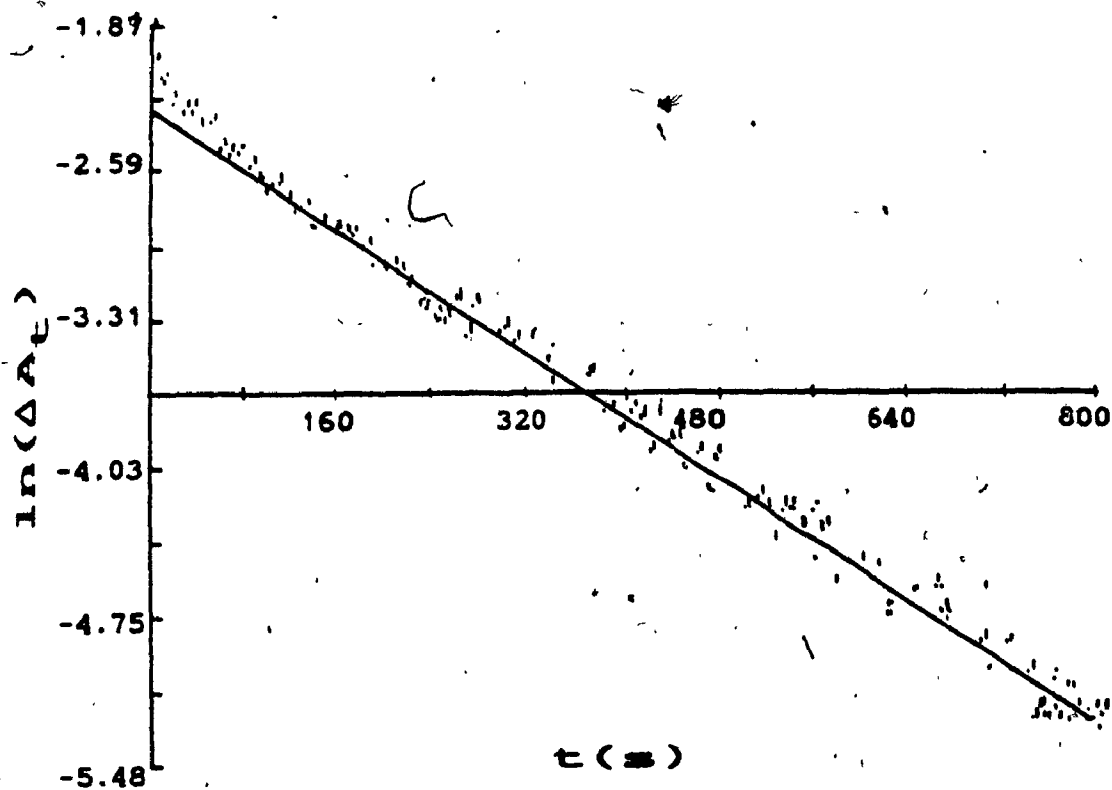


Figure 3.3 Semi-log plot of the data in Figure 3.2 for GCP:CO dissociation.

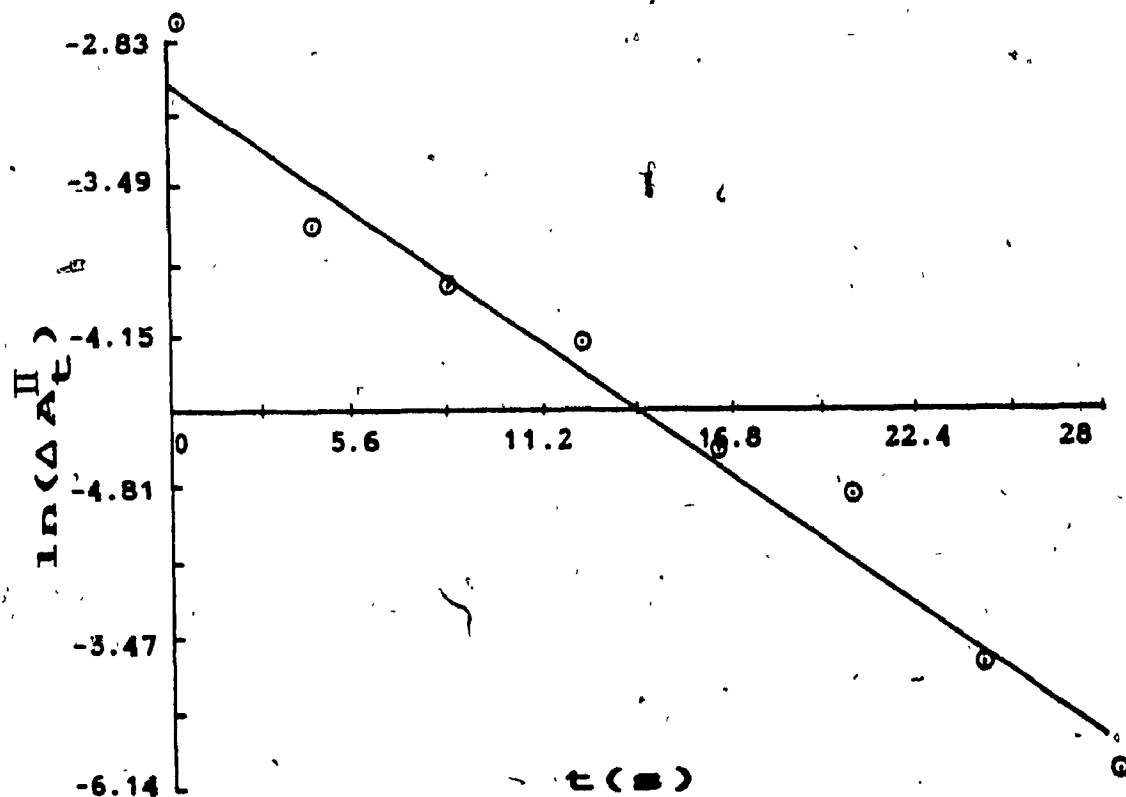


Figure 3.4 Semi-log plot of the data in Figure 3.2 for CCP:CO dissociation over the first 28 s, which corresponds to 3 half lives for the fast phase ($k^{\text{II}} = 7.8 \times 10^{-2} \text{ s}^{-1}$, Table III)

Table III: Thermal Dissociation Rate Constants for CCP:CO and HRP:CO, in the presence of 6% transmittance ND filters, Using NO as a Trap.^a

Protein	P _{CO} (atm)	P _{NO} (atm)	k ^I x 10 ³ b, c (s ⁻¹)	k ^{II} x 10 ² (s ⁻¹)
CCP	0.1	0.1	2.9 ± 0.6	
	1	1	3.5 ± 0.4	7.8 ± 1
HRP	0.1	0.1	2.7 ± 0.7	
	1	1	2.6 ± 0.2	4.5 ± 1

^a 0.01 M Phosphate buffer pH 7.0, 18 ± 0.5°C, [CCP] = 3 μM.

^b At 1 atm CO, the observed kinetics are biphasic and k^I, k^{II} are the rate constants for the slow and fast phases, respectively (Section 2.3).

^c The rate at 0.1 atm CO is equal to the slow phase at 1 atm CO within experimental error. Therefore, both rate constants are labelled k^I.

Table IV: Thermal Dissociation Rate Constant for CCP:CO and HRP:CO in the absence of ND filters, Using NO as a Trap^a.

Protein	P _{CO}	P _{NO}	k ¹ x 10 ³ ^{b, c} (s ⁻¹)	k ¹¹ x 10 ² (s ⁻¹)
CCP	0.1	0.1	5.9 ± 0.7	
	1.0	1.0	4.6 ± 0.6	7.3 ± 0.5
HRP	0.1	0.1	2.9 ± 0.1	
	1.0	1.0	5.8 ± 0.1	2.7 ± 0.1

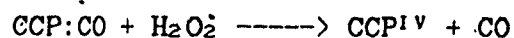
^a 0.01 M Phosphate buffer pH 7.0, 18 ± 0.5°C, [CCP] = 3 μM, a UV cut-off and a 460 nm short pass filter were present.

^{b, c} Refer to footnotes to Table III.

are designated as k^I and k^{II} , respectively. The average values of the rates are reported in Table III. The thermal dissociation rate of CCP:CO was found to be monophasic at 0.1 atm CO since all the absorbance change at 0.1 atm CO, could be accounted for by the slow phase, using ND filters with 10% transmittance (refer to Section 2.3 and Figure 2.2). The magnitude of the rate constant was similar to the magnitude of k^I at 1 atm CO, within experimental error (Table III). NO displacement reactions were also performed in the presence of a UV cut-off and a 460-nm short-pass filter but in the absence of ND filters (Table IV). At 1 atm CO, the kinetics were biphasic while at 0.1 atm CO, only monophasic dissociation could be observed. Comparing the thermal dissociation rate constants of CCP:CO in Tables III and IV, it is found that the magnitudes of k^{II} are similar, in the presence or absence of ND filters. The values of k^I , on the other hand, are greater when ND filter is absent. These results suggest that photoassisted dissociation only affected k^I , the slow thermal dissociation rate constant.

3.2.2 Thermal Dissociation of CCP:CO, using H_2O_2 as a Trap.

H_2O_2 has been used as a trapping agent in CO displacement experiments, in 0.01 M phosphate buffer, pH 7.0. The overall reaction is as follows:



The final product is ferryl CCP ($Fe^{IV} = O$) which is formed upon the two

electron oxidation of reduced CCP. Ferryl CCP has lower absorbance than CCP:CO at 424 nm; thus, monitoring the reaction at this wavelength resulted in an absorbance decay at various CO concentrations. Figure 3.5 shows the absorbance decay at 424 nm when ferryl CCP was formed due to the reaction of CCP:CO with H_2O_2 , at $18 \pm 0.5^\circ\text{C}$. The absorbance decay did not level-off, even at the maximum absorbance change expected for the CO displacement reaction. This was due to the decay of ferryl CCP to ferri-CCP which had a half-life of ~ 30 min. The half-life of the slow component of thermal dissociation was 110 s, which is over 10-fold shorter than ferryl-CCP decay. Analysis of the trace according to Section 2.3, revealed biphasic CO dissociation and the values of the rates are given in Table V. It should be noted that the ND filters were not used to measure the rates of CCP:CO thermal dissociation with H_2O_2 trapping. The UV cut-off (290 nm) filter as well as a 460-nm short-pass filter were present during the course of these measurements.

Comparing the CCP:CO thermal dissociation rate constants, measured in the presence of a UV cut-off and a 460 nm short pass filter, reported in Tables IV and V, it is found that the fast dissociation rate constant (k^{f}) remains essentially the same, when either NO or H_2O_2 are used as trapping agents. The slow dissociation rate constant (k^{s}), however is slightly higher in Table V as compared to k^{f} reported in Table IV, at respective CO pressure. This may be due to the decay of ferryl CCP to ferri-CCP at 424 nm. The biphasic dissociation kinetics at 1 atm CO and monophasic dissociation kinetics at 0.1 atm CO, observed in Table V are in accordance with the NO trapping results reported previously

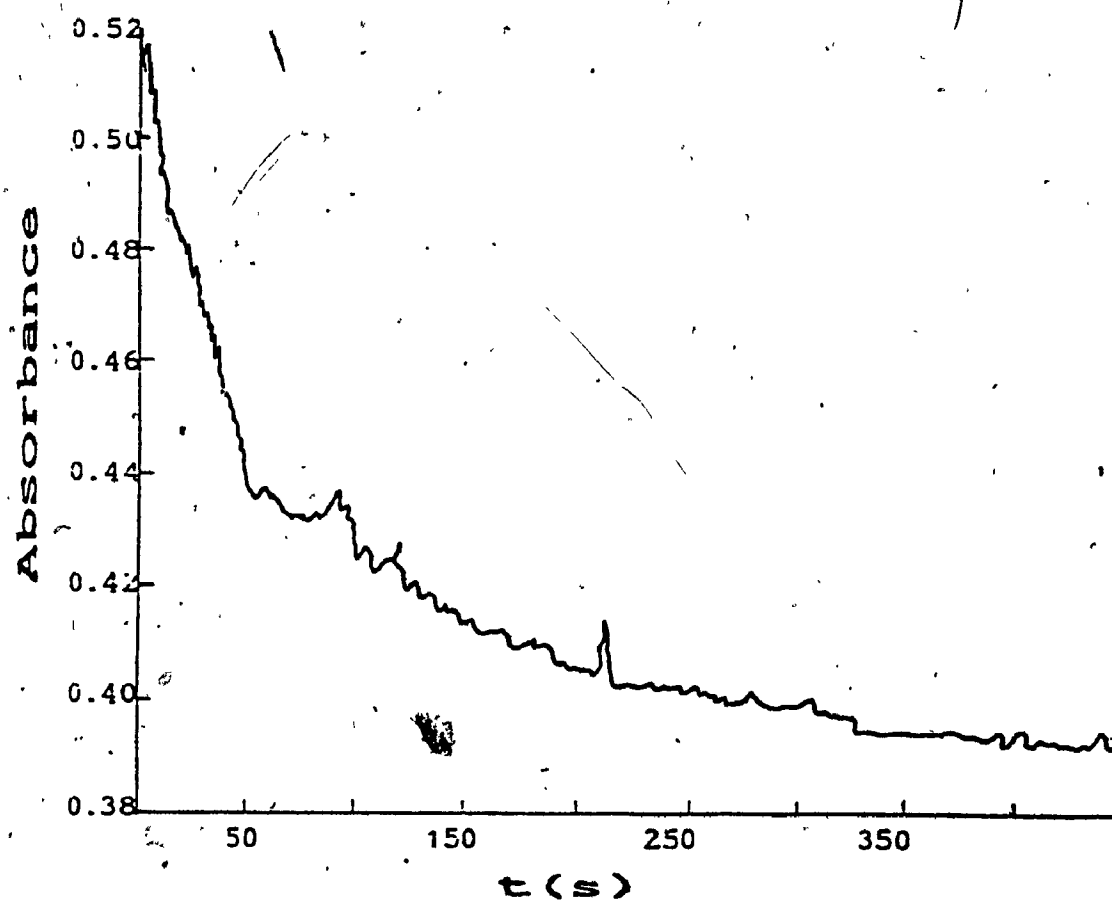


Figure 3.5 Absorbance change at 424 nm due to 3 μM CCP:CO thermal dissociation versus time in 0.01 M phosphate buffer, pH 7.0, using H_2O_2 as a trapping agent, under 1 atm CO.

Table V: Thermal Dissociation Rate Constants for CCP:CO at pH 7.0,
Using H₂O₂ as a Trap^a.

Protein	P _{CO} (atm)	k ¹ x 10 ³ b,c (s ⁻¹)	k ¹¹ x 10 ² (s ⁻¹)
CCP	0.1	6.2 ± 0.1	
	1	7.1 ± 0.4	7.2 ± 0.1

^a 0.01 M Phosphate buffer pH 7.0, 18 ± 0.5°C, [CCP] = 3 μM, no ND filter was present.

^{b,c} Refer to footnotes to Table III.

(Table IV) in the absence of a 6% transmittance ND filter. Photoassisted dissociation seems to affect only the slow component of CCP:CO dissociation reaction.

3.2.3 Thermal Dissociation of HRP:CO at pH 7.0, using NO as a Trap.

In Figure 3.6, spectral changes at 424 nm due to HRP:CO dissociation versus time are shown. The reaction was carried out under 1-atm CO in 0.01 M phosphate buffer, pH 7.0, at $18 \pm 0.5^\circ\text{C}$, using an ND filter with 6% transmittance. Analysis of the absorbance data showed biphasic CO dissociation at 1 atm CO (Figure 3.7 and 3.8) and monophasic CO dissociation at 0.1 atm CO. The average values of the rates are given in Tables III and IV. Comparing Tables III and IV, it can be seen that HRP:CO thermal dissociation does not follow the same trend as that of CCP:CO thermal dissociation, in the presence and absence of ND filters. This is because although the values of k^I are greater in the absence of ND filters, the value of k^{II} has decreased. However, since most of the experiments reported in this study were performed with CCP:CO, the interpretation of the data for HRP:CO thermal dissociation is not attempted.

3.2.4 Thermal Dissociation of CCP:CO at pH 8.0, using NO as a Trap.

In Figure 3.9, the variation in the CCP:CO Soret absorption band between pH 6.6 to 8.0 is shown. The peak maximum shifted from 422.6 at pH 6.6 to 420 nm at pH 8.0, and an isosbestic point was observed at 422 nm.

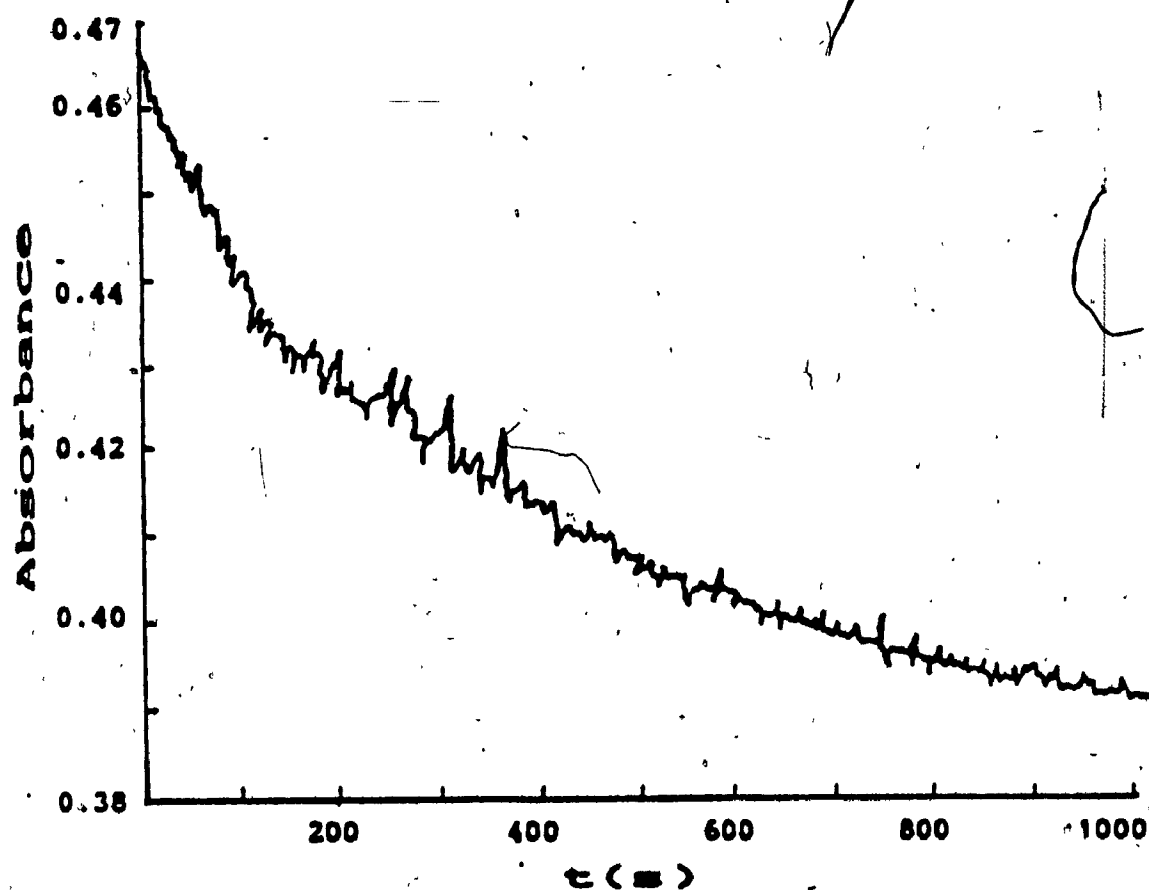


Figure 3.6 Absorbance change at 424 nm due to 3 μ M HRP:CO thermal dissociation versus time in 0.01 M phosphate buffer pH 7.0, at $18 \pm 0.5^\circ\text{C}$, using NO as a trapping agent, under 1 atm CO.

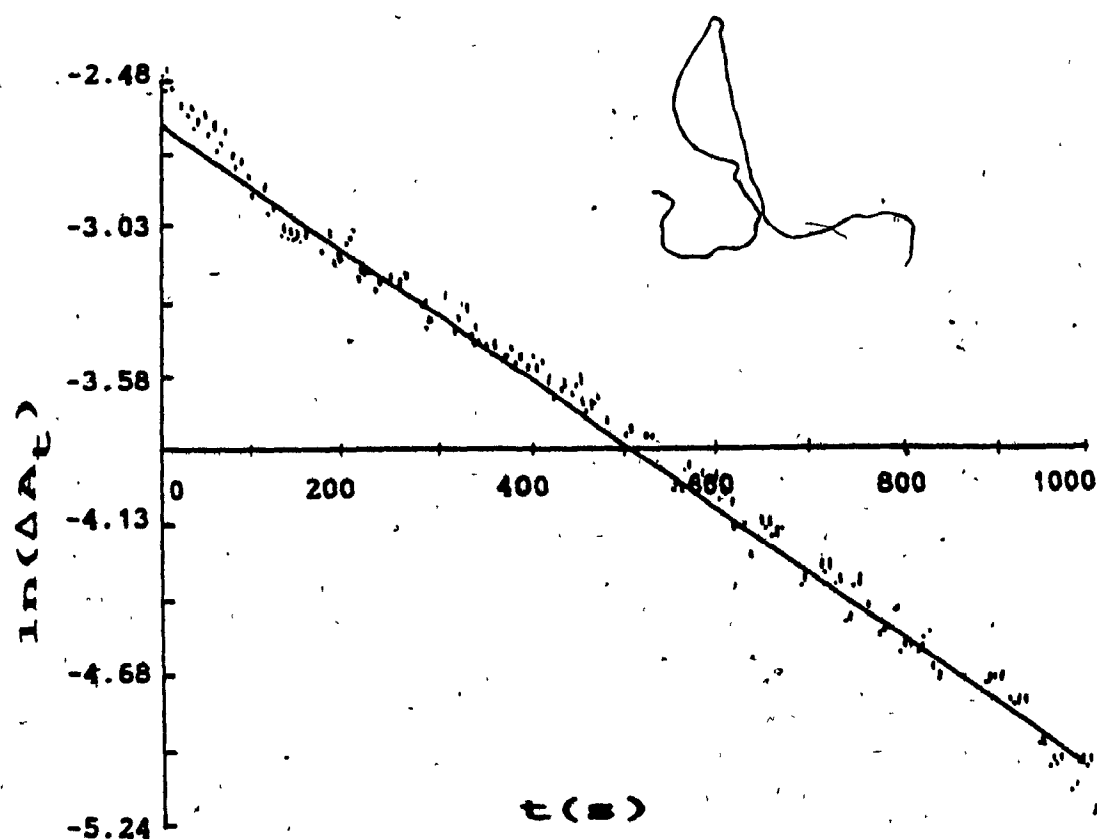


Figure 3.7 Semi-log plot of the data in Figure 3.6 for HRP:CO dissociation.

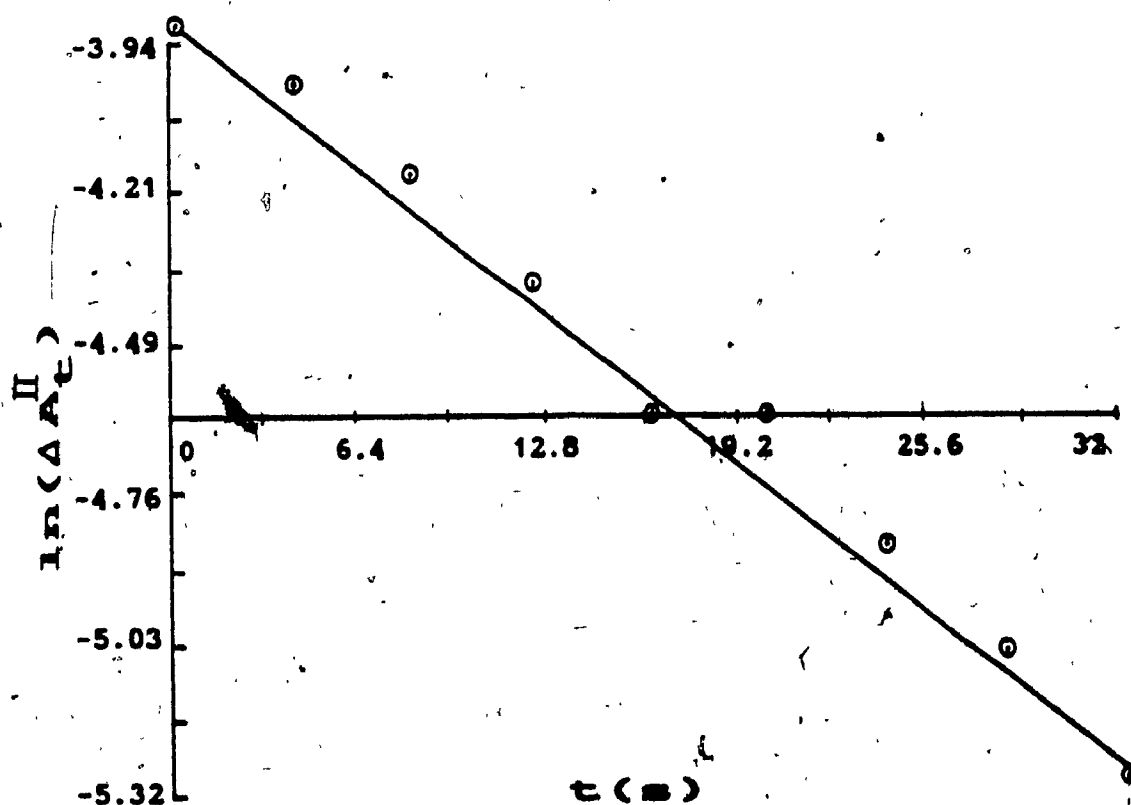


Figure 3.8 Semi-log plot of the data in Figure 3.6 for HRP:CO dissociation over the first 32 s which corresponds to ~ 3 half lives for the fast phase ($k^{\text{II}} = 7.2 \times 10^{-2}$, Table IV).

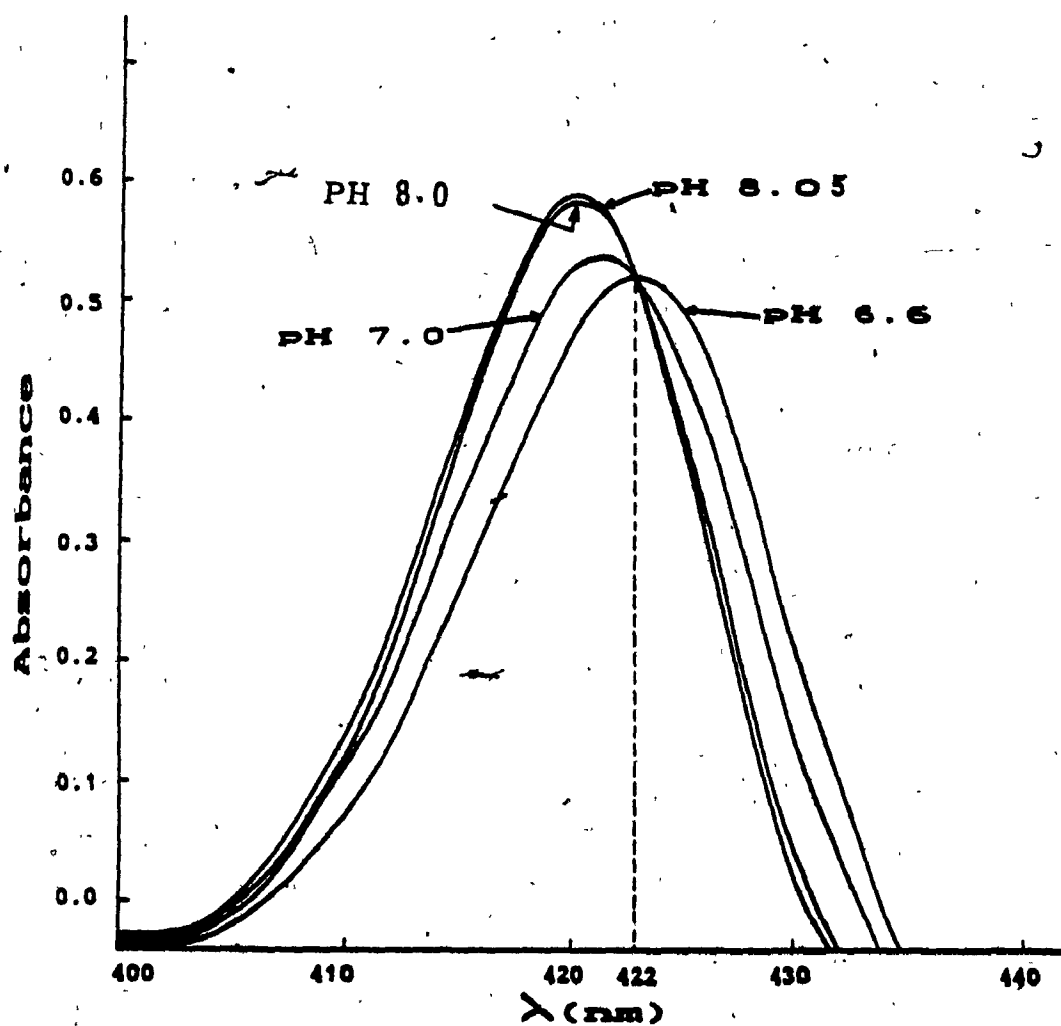


Figure 3.9 Soret absorption spectrum of 2.5 μM CCP:CO at different pH's in 0.01 M phosphate buffer at room temperature. The pH was adjusted by adding 0.2 N NaOH to the cuvette.

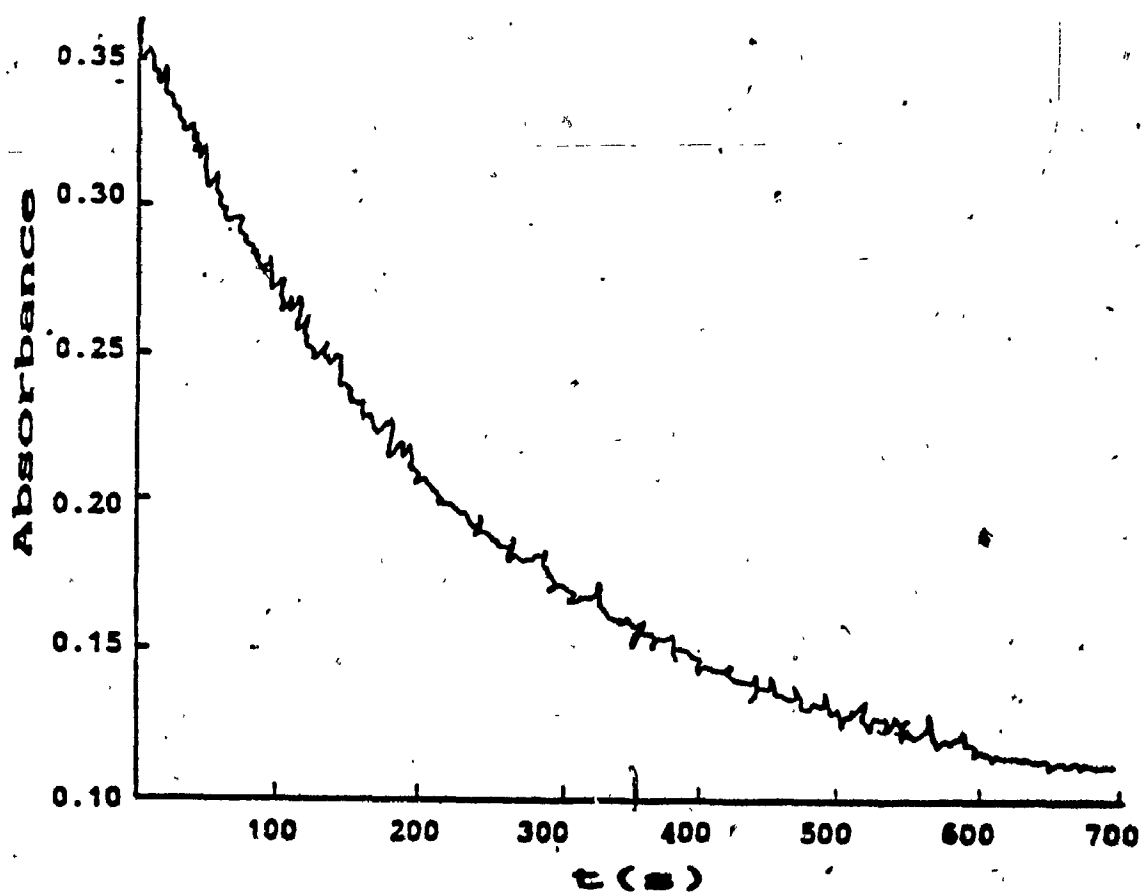


Figure 3.10 Absorbance change at 424 nm due to 3 μ M CCP:CO thermal dissociation versus time. The reaction was carried out in 0.01 M phosphate buffer, pH 8.0, at $18 \pm 0.5^\circ\text{C}$, using NO as a trapping agent. The CO and NO pressures were both 1 atm.

Rates of CCP:CO dissociation in 0.01 M phosphate buffer, pH 8.0, were measured using NO as a trap at $18 \pm 0.5^\circ\text{C}$ (in the presence of 6% transmittance ND filter). Figure 3.10 shows a typical trace of the absorbance decrease versus time at 424 nm under 1 atm CO, and as can be seen from this figure, the thermal dissociation at 1 atm CO is monophasic. The average value of the rate constant $k^{II'}$ was found to be $3.7 \pm 0.3 \times 10^{-3} \text{ s}^{-1}$.

3.2.5 Effect of Phosphate Concentration Upon Fresh CCP:CO Dissociation

Rate Constant at pH 8.0, using NO as a Trap.

The thermal dissociation of fresh CCP:CO was measured in 0.01 and 0.1 M phosphate buffer at pH 8.0 (Figure 3.11). The term "fresh" is used to refer to an enzyme sample which is isolated for less than a week. Smulevich et al. (1986) reported that fresh CCP:CO does not exhibit an acidic to alkaline transition (Form II \rightarrow II') in 0.1 M phosphate buffer at pH 8.0. Hence, we attempted a study of fresh CCP:CO dissociation at 0.01 and 0.1 M phosphate concentration. The results are given in Table VI, and as can be seen from this Table, the CO dissociation rate ($k^{II'}$) was independent of both phosphate and CO concentrations, within experimental error. In these measurements no ND filters were used; however, a UV cut-off and a 460 nm short pass filter were present. Although, these results did not mirror the resonance Raman data (Smulevich et al., 1986), $k^{II'}$ ($\sim 1 \times 10^{-2} \text{ s}^{-1}$) for fresh CCP:CO was ~ 3 -fold greater than $k^{II'}$ ($3.7 \times 10^{-3} \text{ s}^{-1}$) for moderately-

aged CCP (i.e., enzyme which has been isolated for 6 months before use). It should be noted that k_{11}' for moderately aged CCP:CO thermal dissociation was measured in the presence of a 6% transmittance ND filter. However, as mentioned previously no ND filters were used in measurements on the fresh protein, which may serve to increase k_{11}' by a factor of three.

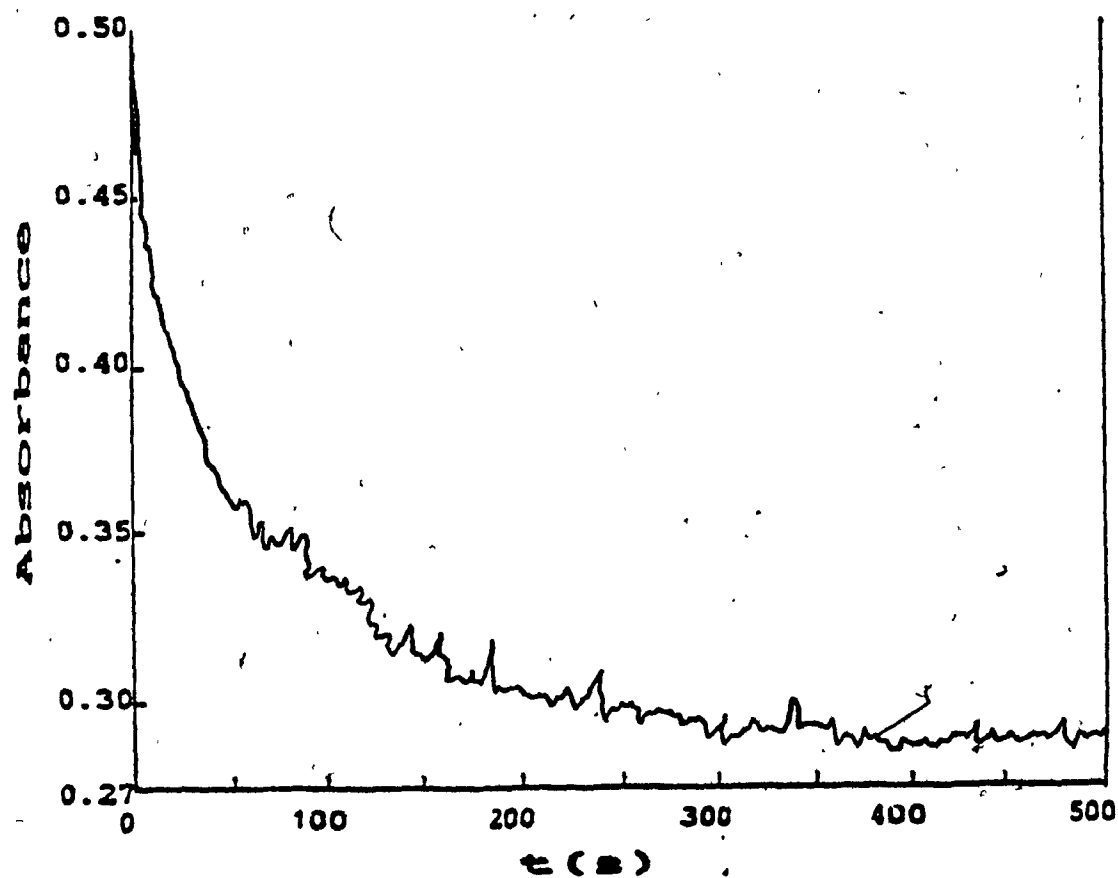


Figure 3.11 Absorbance change at 424 nm due to 2.5 μ M fresh CCP:CO dissociation versus time, in 0.1 M phosphate buffer pH 8.0, at $18 \pm 0.5^\circ\text{C}$, using NO as trapping agent, under 1 atm CO. "Fresh" CCP:CO is defined in Section 3.2.5.

Table VI: Thermal Dissociation Rate Constants for Fresh CCP:CO at pH 8.0, Using NO as a Trap.^a

Phosphate Concentration (M)	P _{CO} (atm)	P _{NO} (atm)	$k^{11} \times 10^2$ ^b (s ⁻¹)
0.01	1	1	1.0 ± 0.1
	0.1	0.1	0.9 ± 0.2
0.1	1	1	1.2 ± 0.01

^a 0.01 M Phosphate buffer, 18 ± 0.5°C. [CCP:CO] = 2.5 μM, no ND filter was present.

^b k^{11} is the thermal dissociation rate constant for alkaline. CCP:CO at pH 8.0.

3.3 Discussion

3.3.1 Thermal Dissociation of CCP:CO and HRP:CO at pH 7.0.

Thermal dissociation rates of CCP:CO and HRP:CO at 1 atm CO are biphasic and yield two distinct rate constants, k^I and k^{II} (Table III). The thermal dissociation kinetics at 0.1 atm CO are monophasic for CCP:CO and HRP:CO, and the magnitude of the rate constants are similar to k^I , within experimental error. These results are in accordance with the findings of Spiro and coworkers who observed alternative CO binding modes to CCP and HRP, using resonance Raman and infrared spectroscopy (Smulevich et al., 1986; Evangelista-Kirkup et al., 1986). On the basis of the resonance, Raman and infrared data (Table II), k^I was assigned to a linear CO adduct (Form I) which is dominant at low pressure and k^{II} was assigned to a tilted CO adduct (Form II) which appears upon increasing the CO pressure.

The presence of biphasic kinetics indicates that for both peroxidases, the CO conformers did not interconvert on the time course of CO dissociation.

Thermal dissociation rates at 1 and 0.1 atm CO using H_2O_2 as a trap (Table V), are also in agreement with the NO displacement results. This means that the kinetics are independent of the trapping agent, and the thermal dissociation rate is biphasic at 1 atm CO and is monophasic at 0.1 atm CO.

The slow rate constants (k^I 's) for CCP:CO and HRP:CO dissociation were similar to that of Mb:CO ($k = 0.005 \text{ s}^{-1}$) and Hb:CO relaxed (R) state ($k = 0.009 \text{ s}^{-1}$) as can be seen in Table I. This suggests that the

bound CO in this case, may not interact with distal-side residues. This interpretation is supported by the vibrational data which revealed a linear mode of CO binding for Form I (Table I) found at low CO pressures. The fast CO dissociation rates (k_{-1}^{II} 's) were similar to those of T-state Hb:CO and strapped hemes (tight strap) where distal-side effects have been shown to be present (Ward et al., 1981). The fast CO dissociation rates were only observed at high CO pressures where according to Smulevich et al. (1986), the bound CO is tilted and H-bonded to distal residues. Hence, it seems that upon increasing the CO

pressure, the distal-side residues interact with the bound ligand and tilt it. This tilting process leads to increased instability of the Fe-CO bond and results in the observed values reported in Tables III and V. Traylor et al. (1981) measured the kinetic, equilibrium and associated thermodynamic values for CO reactions with chelated hemes (chelated hemes have strain built into the proximal side). Their results suggested that proximal strain results in nearly equal change in association and dissociation rates whereas distal side steric effects only affect the association rates. Therefore, the observed differences between Form I and Form II, of CCP:CO and HRP:CO dissociation rate constants, according to Traylor, suggests the involvement of proximal side residues. Recently, Coletta et al., 1986 measured CO dissociation and association rate constants to ~~HRP~~^{II}, at very low CO concentrations ($< 1 \mu\text{M}$). In their study, the value of equilibrium constant measured, directly was similar to that obtained kinetically. The pH dependence of CO dissociation rate constant between pH 3-5 led them to suggest the

role of the heme propionates, located in the proximity of the heme, in the control of the heme-CO dissociation process. However, their value of the HRP:CO thermal dissociation constant at 20°C ($1.1 \times 10^{-4} \text{ s}^{-1}$) is approximately 30 fold less than the slow HRP:CO dissociation rate constant, k^1 in this study ($3.5 \times 10^{-3} \text{ s}^{-1}$). This difference may very well be due to the effect of their experimental conditions, which were quite different from those used in our study. For example Coletta and coworkers measured the rate constants at 0.1 M phosphate buffer and used O_2 as trapping agent, whereas we used NO and H_2O_2 as trapping agents and always worked with 0.01 M phosphate buffer. Also, the CO concentrations during the course of this study were within the range of 3000-30 μM which were always at least 10 fold higher than the CO concentrations used by Coletta et al., 1986. The dependence of the HRP:CO thermal dissociation rate constant on CO concentration is in agreement with various CO binding modes to peroxidases at 0.1 atm and 1 atm CO, have already been reported (Evangelista-Kirkup et al., 1986; Smulevich et al., 1986). The fact that HRP:CO thermal dissociation rate constant at pH 3.25 at 20°C, reported by Coletta et al., 1986, is quite similar to the slow HRP:CO dissociation (k^1) in our study, could suggest that we performed NO trapping experiments at pH's lower than 7. However, NO in the presence of traces of O_2 oxidizes to HNO_3 , which may serve to use up the buffering capacity of 0.01 M phosphate buffer and could have resulted in lower pH's in our experiments. Therefore, considering all of the above factors we conclude that the differences between our thermal dissociation rate constants and those reported by Coletta et

al., 1986 may be due to the differences between experimental conditions in our study as compared to theirs.

3.3.2 Thermal Dissociation of CCP:CO at pH 8.0, using NO as a Trap.

The CCP:CO thermal dissociation kinetics in 0.01 M phosphate buffer pH 8.0 were monophasic. This is in accordance with resonance Raman and infrared data, which provides evidence for the presence of a single CO conformer at alkaline pH. According to Smulevich et al. (1986) this new conformer (Form II') is tilted similar to Form II, but is not H-bonded to distal residues. The high value of $\nu(\text{CO})$ observed by the resonance Raman and infrared study reported in Table II supports the above statements. Based on these findings, one possibly expects to observe similar kinetic behaviour between Form II and II', since they are both tilted, and both forms should therefore be destabilized. But Form II' dissociation rate was $3.7 \pm 0.3 \times 10^{-3} \text{ s}^{-1}$ which was 20-fold lower than the corresponding value for Form II which was $7.8 \pm 0.1 \times 10^{-2} \text{ s}^{-1}$.

3.3.3 Effect of Phosphate Concentration on Thermal Dissociation of

CCP:CO

Smulevich et al. (1986), reported that in 0.1M phosphate buffer, conversion of Form II \rightarrow II' at pH 8.0 is inhibited in fresh CCP:CO. The results in Table VI show that the kinetic behaviour of the fresh CCP:CO complex at pH 8.0, does not change with increasing the phosphate concentration. A single dissociation rate constant is observed in (0.01 M and 0.1 M phosphate concentration, which is also independent of

CO concentration. The fresh CCP:CO dissociation rate constant at pH 8.0 is 3-fold greater than that of aged CCP:CO at the same pH, and its magnitude is very close to that of R-state Hb:CO. Hence, it is possible that like native CCP (Yonetani and Anni, 1987) aging also leads to structural changes in CCP:CO. However, it should be mentioned again here that no ND filters were used in the studies of fresh CCP:CO, but were used in those on moderately aged CCP:CO (Sections 3.2.4 and 3.2.5). Therefore, the possibility of photoassisted dissociation has not been ruled-out for fresh CCP:CO.

CHAPTER 4

REACTIONS OF CCP:CO WITH FERRICYTOCHROME c's FROM YEAST AND

HORSE HEART

4.1 Introduction

Gel filtration (Kang et al., 1977; Mochan, 1970) sedimentation velocity (Mochan and Nicholls, 1971), chemical shifts of NMR resonances of cytochrome c (Gupta and Yonetani, 1973), and quenching of fluorescence of modified CCP by cytochrome c (Leonard and Yonetani, 1973) indicated that cytochrome c binds to the peroxidase in solution.

The equilibrium association constant for the complex had been determined as a function of the ionic strength and varied between $6 \pm 3.6 \times 10^6 \text{ M}^{-1}$ and $2.2 \pm 1.9 \times 10^3 \text{ M}^{-1}$ over the ionic strength range of 0.01 M to 0.2 M (Erman and Vitello, 1980).

Cytochrome c should also bind to the CCP:CO complex. Mochan and Nicholls (1971) found that the rate of reaction of CCP with H_2O_2 is unaffected in the presence of cytochrome c. Therefore in C/CCP complex a channel leading from the external medium to the heme in CCP must remain open (Poulos et al., 1978). Hence, it is expected that the presence of cytochrome c would not interfere with the CO ligation of CCP^{Fe} .

Intramolecular electron transfer rates between ferricytochrome c and CCP^{Fe} have been measured directly by Cheung et al., 1986. The electron transfer rate between horse heart ferricytochrome c and CCP was found to be $0.23 \pm 0.02 \text{ s}^{-1}$. Variations in the primary structure of cytochrome c cause changes in the intramolecular electron transfer rate. For example

the intramolecular electron transfer rate when yeast cytochrome c is used is 1.7 s^{-1} which is an order of magnitude higher than the corresponding value for horse heart cytochrome c. These results are supported by a report given by Ho et al. (1985) on excited state reactions of cytochrome c/CCP. Based on these findings the reactions of horse heart and yeast ferricytochrome c with CCP:CO were predicted to occur according to the Scheme below in the following sections.



4.2 Results

4.2.1.1 Reaction of Horse Heart Ferricytochrome c with CCP:CO at 1 atm CO.

Figure 4.1, shows the Soret absorption spectra of CCP^{III} and CCP:CO in 0.01 M phosphate buffer pH 7.0, at room temperature. A clear isosbestic point could be observed at 414 nm. The extinction coefficients of oxidized and reduced horse heart cytochrome c at 414 nm are 97 and $124 \text{ mM}^{-1} \text{ cm}^{-1}$, respectively (Margoliash and Prohvirt, 1959); therefore, the absorbance increase which occurred during the above reaction at 414 nm was only due to the reduction of cytochrome c.

Figure 4.2 shows the absorbance change at 414 nm due to the reaction of horse heart c with CCP:CO in 0.01 M phosphate buffer pH 7.0 at $18 \pm 0.5^\circ\text{C}$ under 1 atm CO, using a 13% transmittance ND filter.

The absorbance change versus time was analysed according to Section 2.3 and the kinetics were found to be biphasic at 1 atm CO (Figure 4.3

and 4.4). The rate of the fast and slow components were ~ 4-fold and ~ 2-fold slower than the respective fast and slow rate constants in the NO trapping experiments (Table III), and therefore are designated k^{II} and k^I , respectively. The average values of the rates are reported in Table VII.

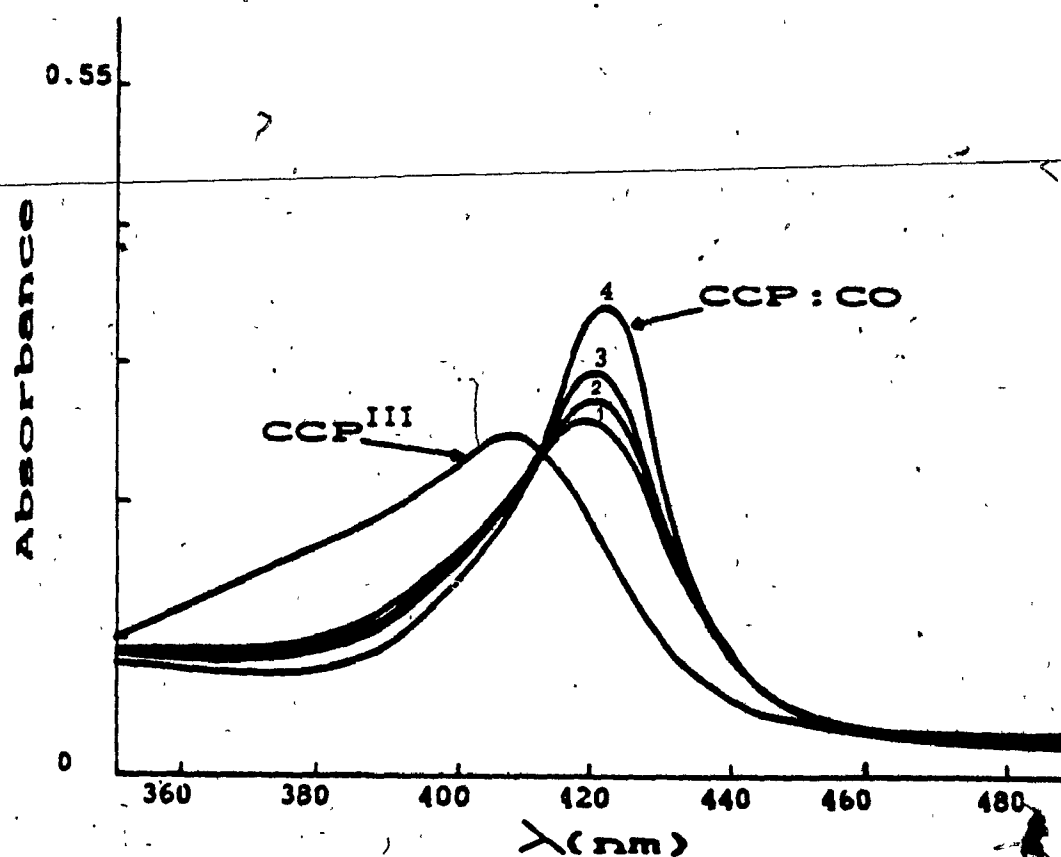


Figure 4.1 Soret absorption spectrum of $2.5 \mu\text{M}$ CCP^{III} and $2.5 \mu\text{M}$ CCP:CO in 0.01 M phosphate buffer pH 7.0, at room temperature (Traces 1-4 were obtained after 2, 4, 6, and 8 s exposure of CCP^{III} samples to UV light respectively, in order to form CCP:CO . The absorption of CCP:CO remained constant after 8 s and resembles trace 4).

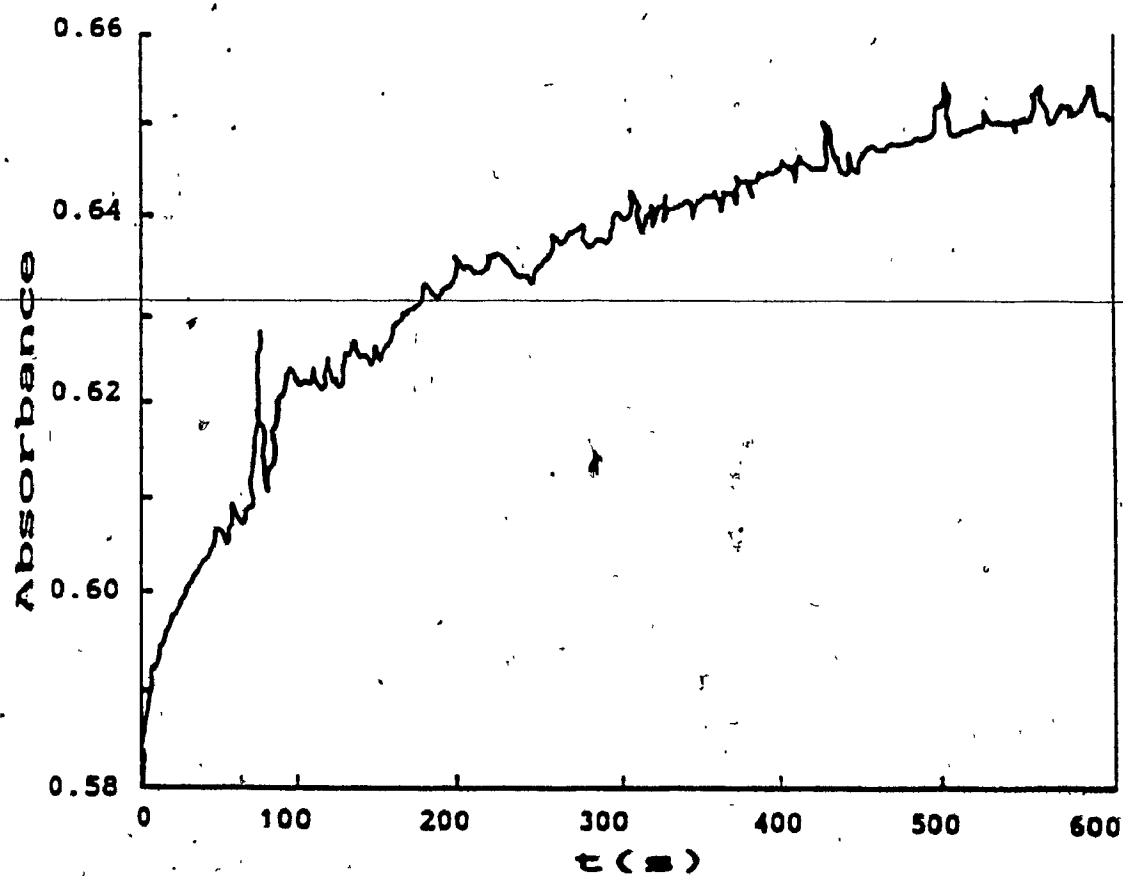


Figure 4.2 Absorbance change at 414 nm due to the reaction of 2.5 μ M CCP:CO with ferricytochrome c in 0.01 M phosphate buffer pH 7.0, under 1 atm CO.

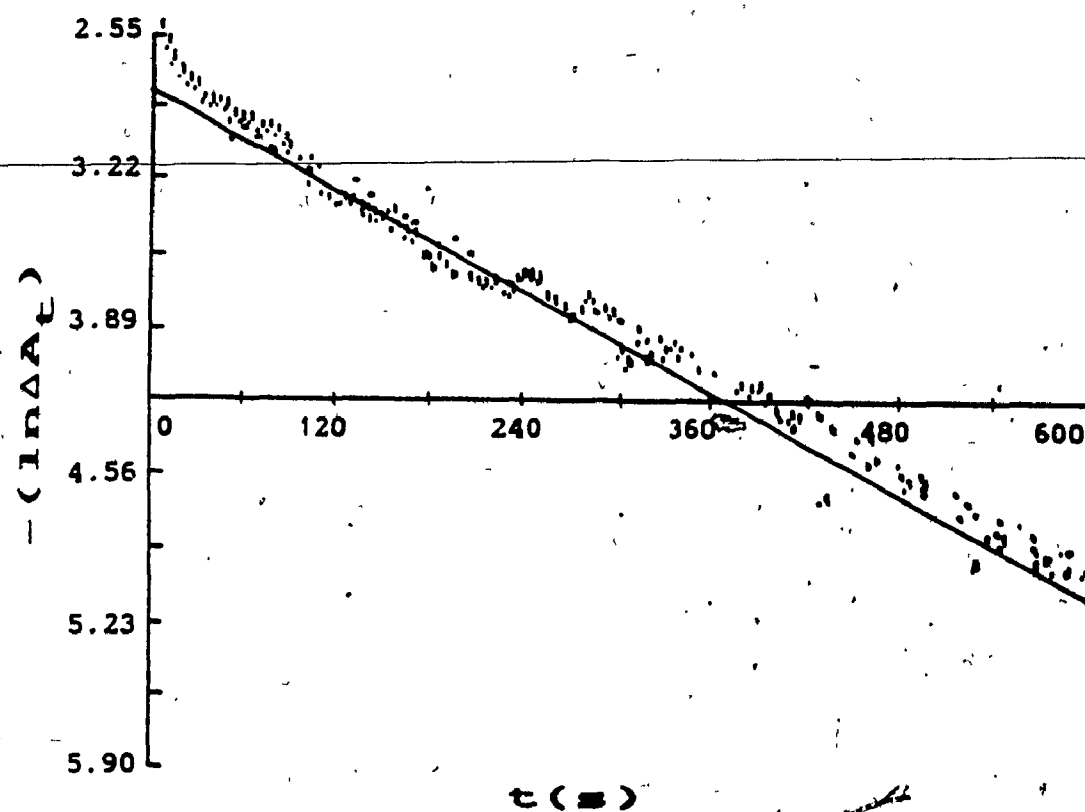


Figure 4.3 Semi-log plot of the data in Figure 4.2 for the reaction of horse heart ferricytochrome c and CCP:CO.

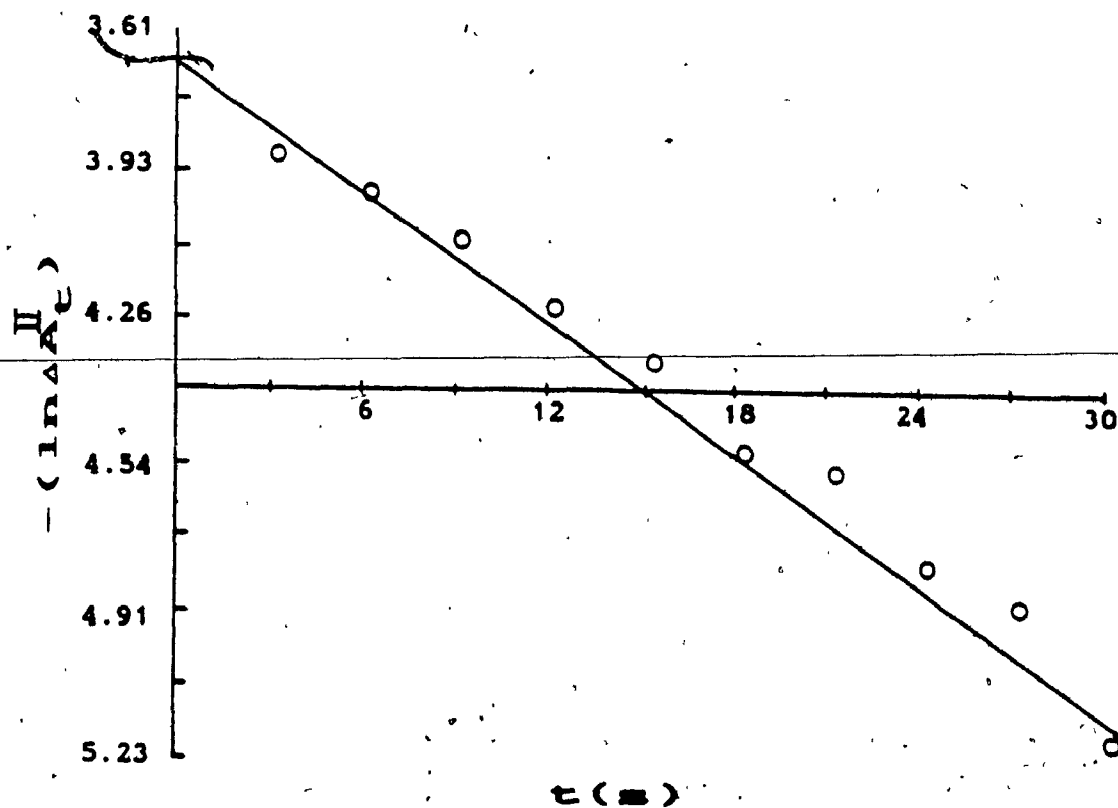


Figure 4.4 Semi-log plot of the data in Figure 4.2 for the reaction of horse heart ferricytochrome c and CCP:CO over the first 30 s. This corresponds to ~ 0.9 half lives of the fast phase ($k^{II} = 2.0 \times 10^{-2} \text{ s}^{-1}$, Table VII).

Table VII: Rate Constants for the Reaction of Ferricytochrome c's
with CCP:CO at 1 atm CO^a.

Ferricytochrome C	$k^{II} \times 10^2$ ^b (s ⁻¹)	$k^I \times 10^3$ ^c (s ⁻¹)
Yeast	3.0 ± 0.8	3.0 ± 0.7
Horse Heart	2.0 ± 0.2	1.3 ± 0.5

^a 0.01 M phosphate buffer pH 7.0, $18 \pm 0.5^\circ\text{C}$, [CCP] = 2.5 μM , a 13% transmittance ND filter was present.

^{b, c} At 1 atm CO, biphasic kinetics are observed and k^I and k^{II} refer to the rate constants of the slow and fast phase, respectively,

4.2.1.2 Temperature Dependence of the Reaction Rate of Horse Heart

Ferricytochrome c with CCP:CO.

The temperature dependence of the reaction between horse heart ferricytochrome c and CCP:CO was studied in 0.01 M phosphate buffer, pH 7.0, from 6.5°C to 32°C. Absorbance change with time was analysed according to section 2.3. At each temperature, the absorbance change was found to be biphasic, over the temperature range studied. As can be seen in Table VIII, the rate constant for the fast component (k^1) was independent of the temperature. The average value of k^1 is $6.2 \pm 0.4 \times 10^{-2} \text{ s}^{-1}$. The slow component, however, increased linearly with temperature (Table IX). Thermodynamic parameters for this component were determined using the Eyring expression:

$$\ln k^1/T = \ln k/h - \Delta H^\circ/RT + \Delta S^\circ/R$$

where k = Boltzmann's constant, h = Planck's constant, T = absolute temperature, ΔH° = enthalpy of activation and ΔS° = entropy of activation.

The Eyring expression predicts that a plot of $\ln k^1/T$ versus $1/T$ will be linear and the slope and the intercept will yield the enthalpy and entropy of activation respectively. The data in Table IX are plotted in Figure 4.5 and a straight line with a correlation coefficient of 0.990 was obtained. The enthalpy and the entropy of activation are 6.4 Kcal mol^{-1} and -47 e.u., respectively. It should be noted that in the above measurements no ND filters were used, however a 290 nm cut-off filter as well as a 460 nm short-pass filter were present.

Table VIII : Observed Rate Constants (k^{II}) for the Fast Phase of the Reaction Between Horse Heart Ferricytochrome c and CCP:CO, versus temperature at 1 atm CO^a.

T (°C)	$k^{II} \times 10^2$ (s ⁻¹)
6.5	6.02 ± 0.02
9.2	6.69 ± 0.007
17.0	5.50 ± 0.02
20.0	6.7 ± 0.005
25.0	5.9 ± 0.05
32.0	6.3 ± 0.04

^a 0.01 M phosphate buffer pH 7.0, [CCP] = 2.5 μ M; an ND filter was not utilized.

Table IX: Observed Rate Constants for the Slow Phase of the Reaction
Between Horse Heart Ferricytochrome c and CCP:CO versus
temperature at 1 atm CO^a.

T (°C)	$k^1 \times 10^3$ (s ⁻¹)	$1/T \times 10^3$ (K ⁻¹)	$\ln(k^1/T)$
6.5	2.8 ± 0.5	3.58	-11.55
9.2	3.5 ± 0.4	3.54	-11.30
17.0	4.5 ± 0.1	3.45	-11.07
20.5	4.7 ± 0.1	3.41	-11.03
25.0	6.1 ± 0.3	3.36	-10.80
32.0	8.3 ± 0.8	3.28	-10.51

^a Refer to footnote to Table VIII

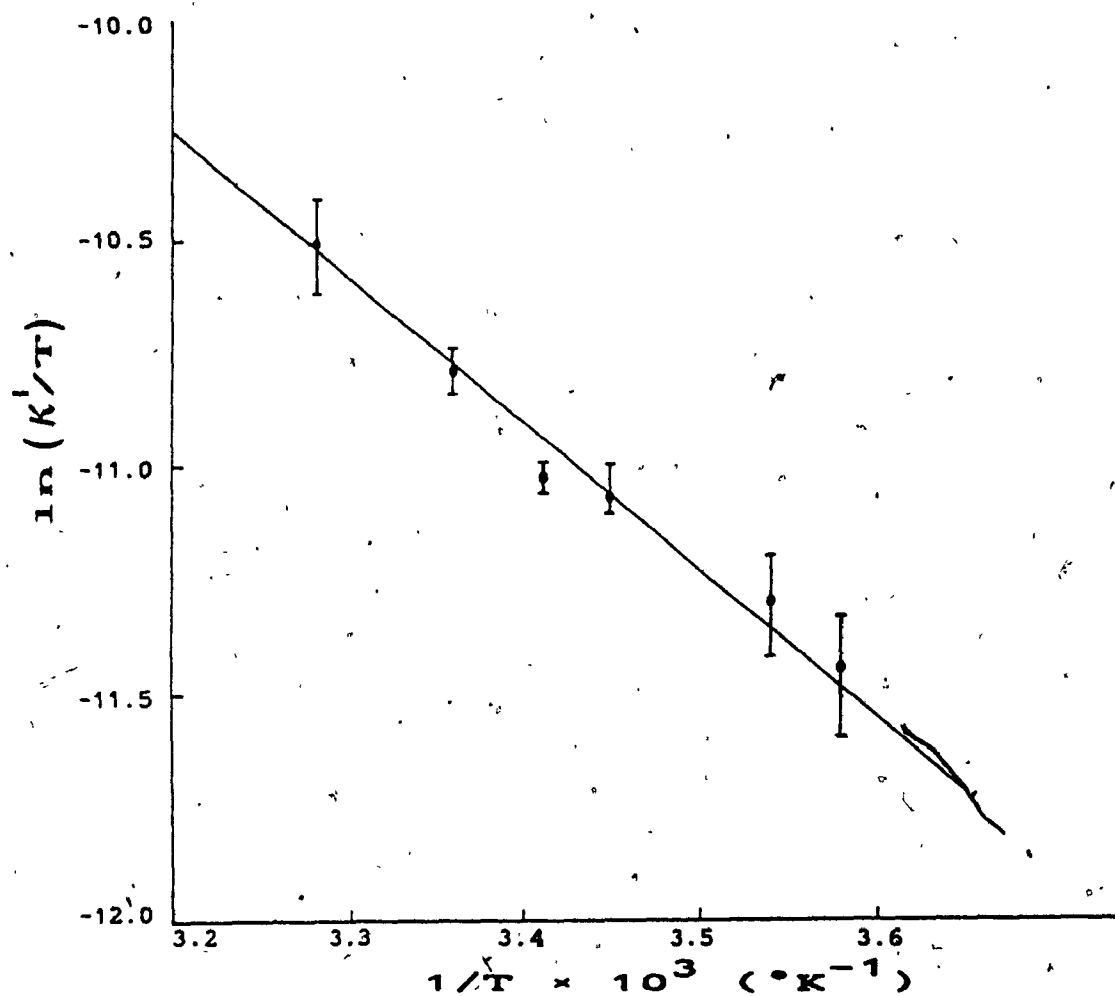


Figure 4.5 Temperature dependence of the observed rate constants for the slow phase of horse heart ferricytochrome c and CCP:CO reaction in 0.01 M phosphate buffer pH 7.0, under 1 atm CO.

Table X: Activation Parameters for CO Dissociation from Mb:CO,
and HRP:CO^a

Protein	ΔH^\ddagger Kcal mole ⁻¹	ΔS^\ddagger e.u.
Mb ^b	26	25
HRP ^{c, d}	34	38

^a 0.01 M phosphate buffer pH 7. The values of k were taken from the literature. $\ln(k/T)$ versus $1/T$ were plotted for the CO dissociation rate constant from Mb:CO and HRP:CO. The activation parameters for the CO dissociation reaction were calculated from the slope and the intercept of the first order fit to the data points for respective protein.

^bWittenberg et al., 1967

^cWittenberg et al., 1965

^dColetta et al., 1986 found that ΔH^\ddagger is equal to 27 kcal mol⁻¹ for HRP:CO thermal dissociation at pH 7.0.

4.2.2 Reaction of Yeast Ferricytochrome c with CCP:CO at 1 atm CO.

Yeast ferricytochrome c was reacted with CCP:CO in the presence of 13% transmittance ND filter in 0.01 M phosphate buffer, pH 7.0, at $18 \pm 0.5^\circ\text{C}$ to yield the reduced cytochrome c and oxidized CCP. This reaction was also monitored at 414 nm. In Figure 4.6, absorbance changes due to the above reaction versus time can be seen, using a 13% transmittance ND filter. The end of the reaction was determined by obtaining a peak at 416 nm corresponding to C^{II} of exactly the same concentration as C^{III} originally added to the cuvette. Data analysis according to section 2.3 revealed biphasic kinetics (Figure 4.7 and 4.8) and the magnitude of the rates are given in Table VII.

4.2.3 Reaction of Horse Heart and Yeast Ferricytochrome c's with CCP:CO at 0.1 atm CO.

Reaction of horse heart ferricytochrome c with CCP:CO was also measured at 0.1 atm CO, in 0.01 M phosphate buffer, pH 7.0, at $18 \pm 0.5^\circ\text{C}$, using a 13% transmittance ND filter (Figure 4.9). Absorbance changes versus time were analysed as previously explained in Section 2.3 and were found to be monophasic. The rate constant (k^{I}) was the same as k^{I} for this reaction at 1 atm CO (Table XI). The reaction of yeast ferricytochrome c with CCP:CO under 0.1 atm CO (Figure 4.10) was also found to be monophasic. However, the rate constant k , in this instance (Table XI) was found to be the intermediate between k^{I} and k^{II} for yeast cytochrome c in Table VII.

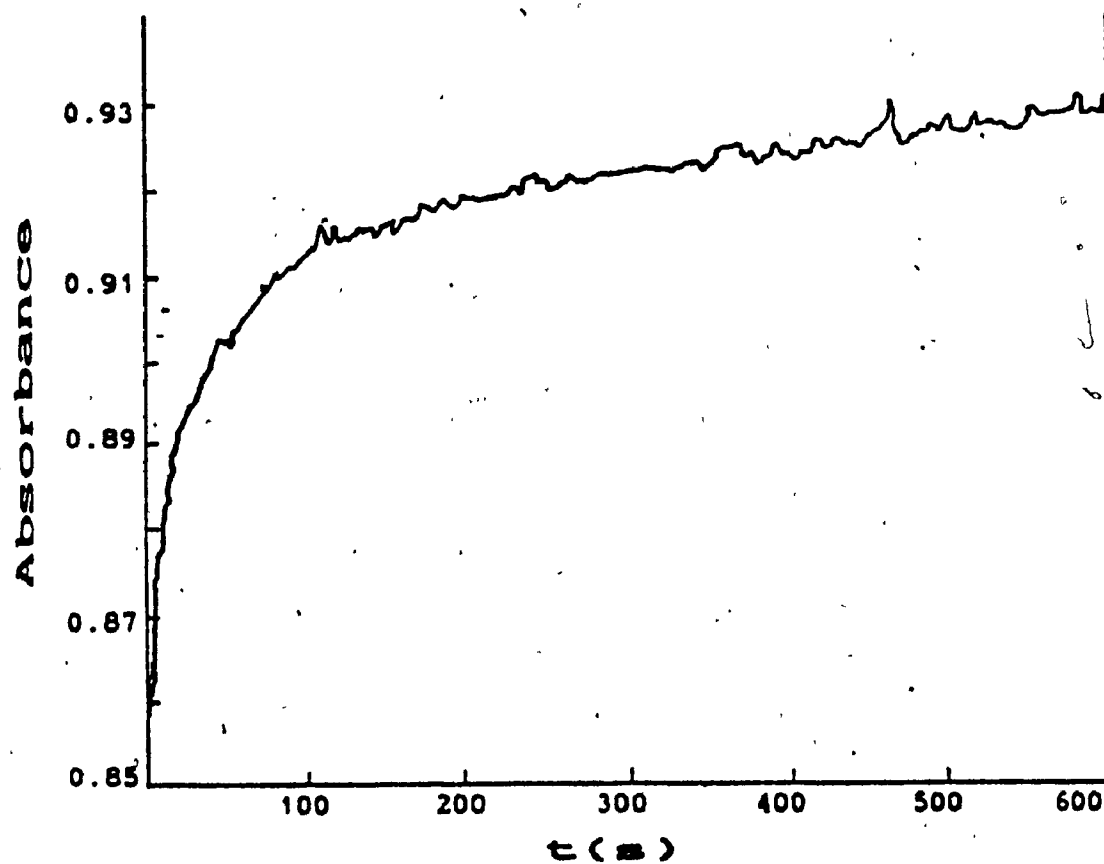


Figure 4.6 Absorbance change at 414 nm due to the reaction of yeast ferricytochrome c with CCP:CO in 0.01 M phosphate buffer pH 7.0, at $18 \pm 0.5^\circ\text{C}$, under 1 atm CO.

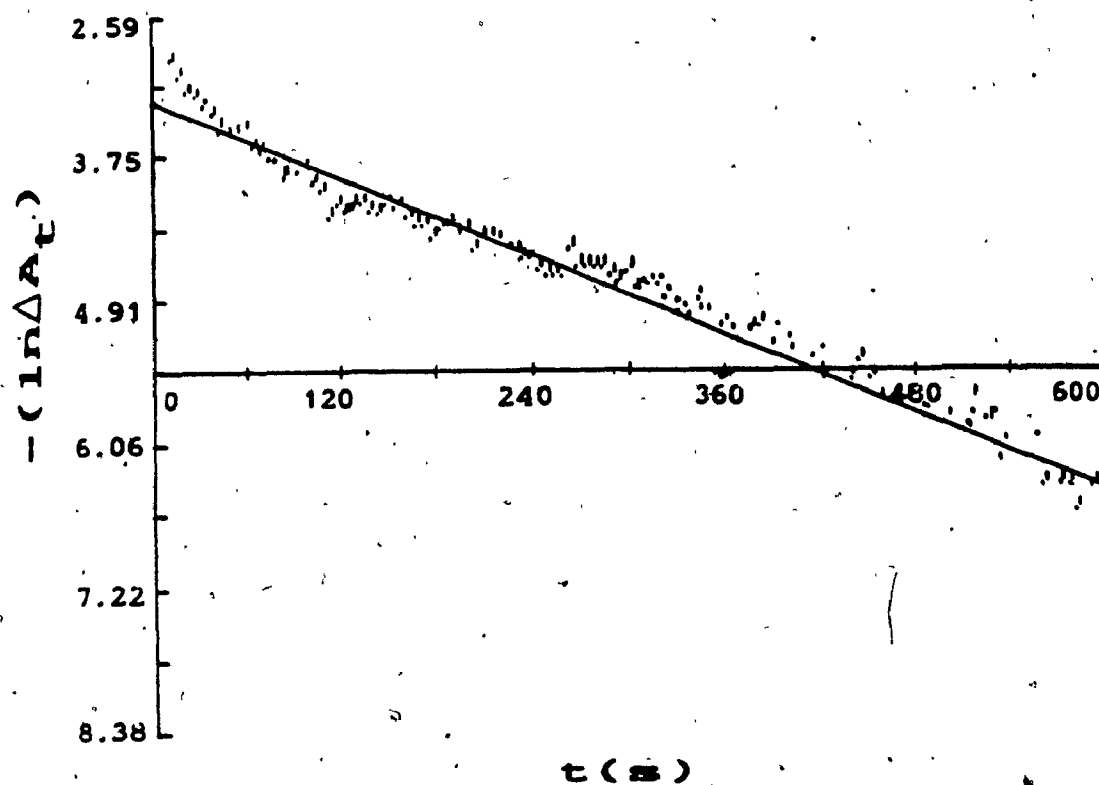


Figure 4.7 Semi-log plot of the data in Figure 4.6 for the reaction of yeast ferricytochrome c and CCP:CO.

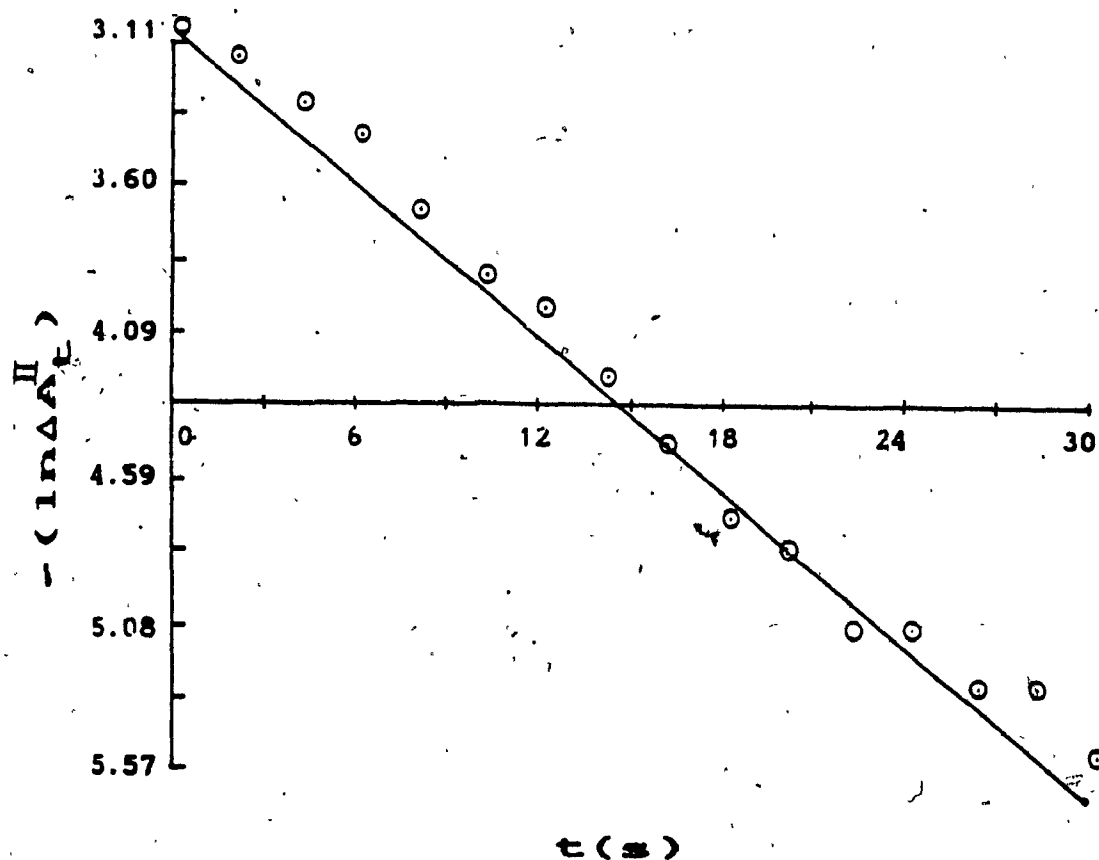


Figure 4.8 Semi-log plot of the data in Figure 4.6 for the reaction of yeast ferricytochrome c with CCP:CO over the first 30 s. This corresponds to 1.3 half lives of the fast phase ($k^{\text{II}} = 3.0 \times 10^{-2} \text{ s}^{-1}$, Table VII).

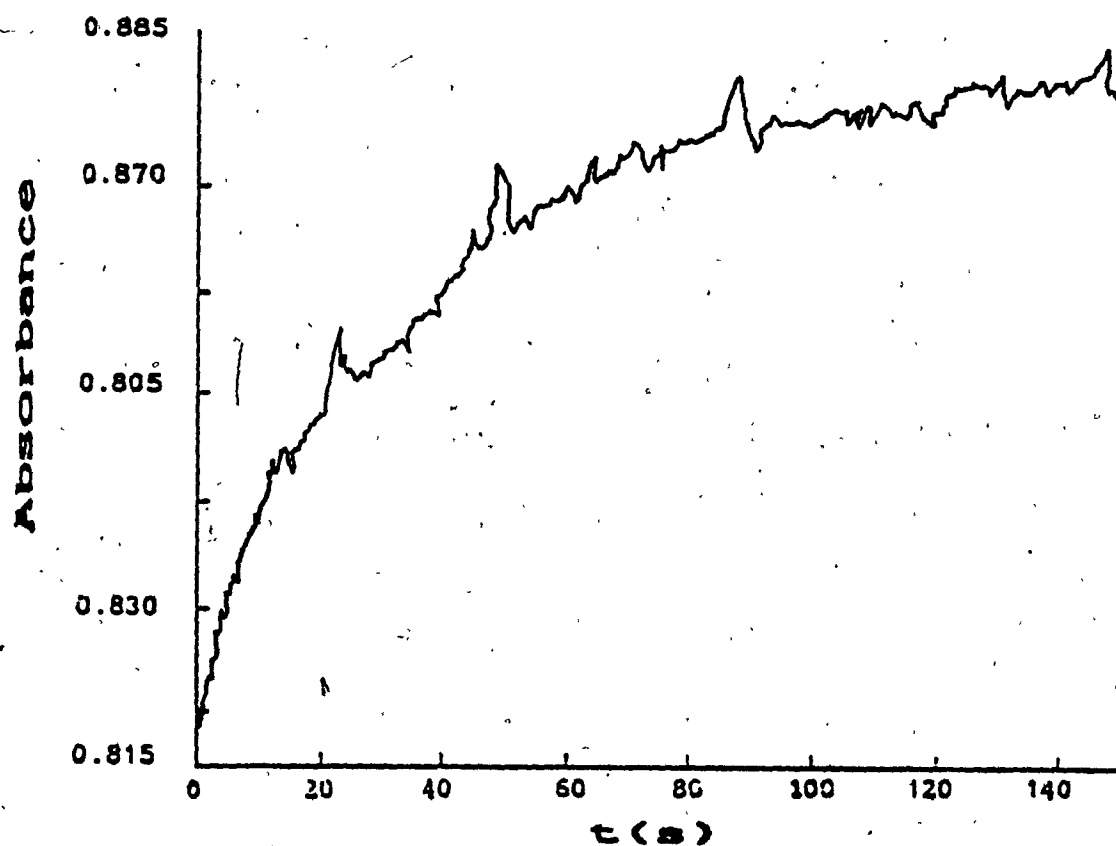


Figure 4.9 Absorbance change at 414 nm due to the reaction of horse heart ferricytochrome c with CCP:CO versus time in 0.01 M phosphate buffer pH 7.0, at $18. \pm 0.5^{\circ}\text{C}$, under 1 atm CO.

Table XI: Rate Constants for the Reactions of Horse Heart and Yeast
 Ferricytochrome c's with CCP:CO at 0.1 atm CO^a.

Ferricytochrome	$k \times 10^2$	$k^1 \times 10^3$ ^b
c	(s ⁻¹)	(s ⁻¹)
yeast	1.0 ± 0.06	-
horse heart	-	1.5 ± 0.4

^a 0.01 M phosphate buffer pH 7.0, $18 \pm 0.5^\circ\text{C}$, [CCP] = 2.5 μM , a 13% transmittance ND filter was present.

^bThe Rate Constant for the reaction of horse heart ferricytochrome c is the same as k^1 in Table VII and therefore also labelled k^1 .

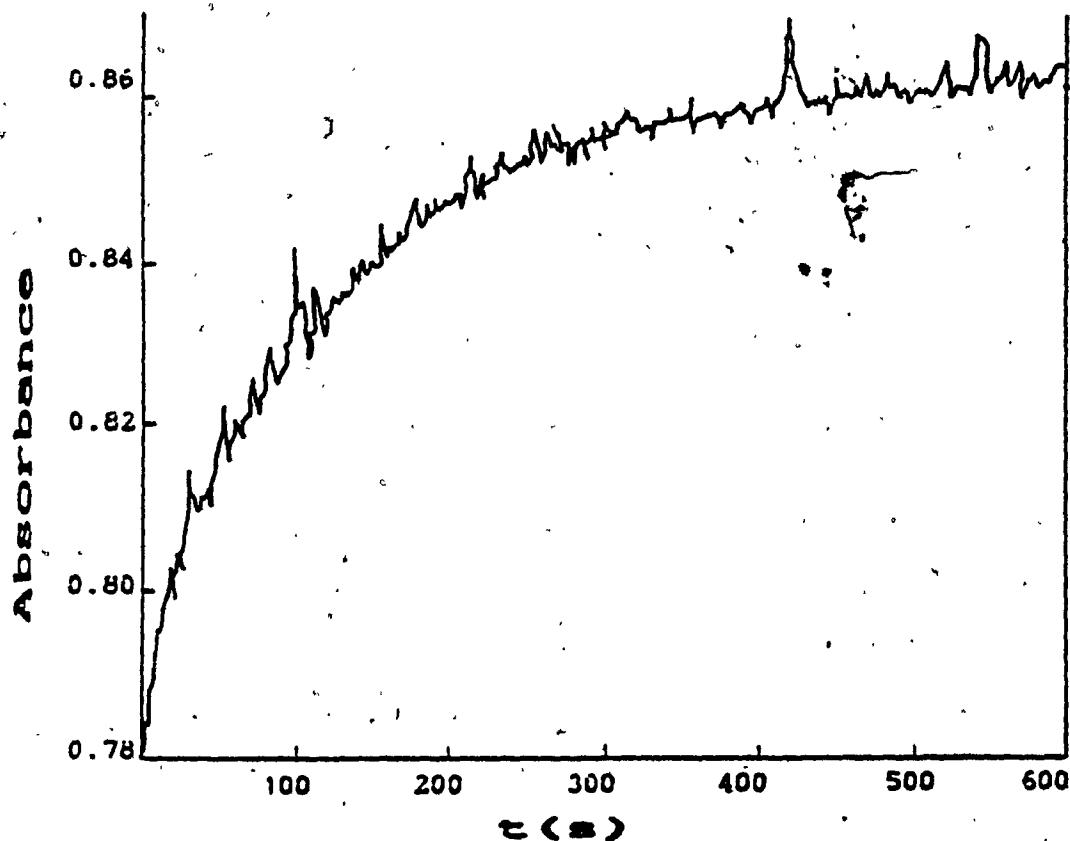


Figure 4.10 Absorbance change at 414 nm for the reaction of yeast ferricytochrome c with CCP:CO versus time in 0.01 M phosphate buffer pH 7.0, at $18 \pm 0.5^\circ\text{C}$ under 0.1 atm CO.

4.2.4 Thermal Dissociation of CCP:CO in the Presence of Yeast and Horse Heart Ferrocyanochrome c's Using NO as a Trap.

Rate of CCP:CO dissociation was measured in the presence of Ferrocyanochrome c's using NO as a Trap. The CO pressure was 0.05 atm and the reaction was performed in 0.01 M phosphate buffer, pH 7.0, at $17 \pm 0.5^\circ\text{C}$. The reaction is assumed to have occurred as follows:



Figure 4.11 shows the absorbance changes due to CO dissociation reaction in the presence of yeast ferrocyanochrome c. It was found that CCP:CO dissociation in the presence of yeast ferrocyanochrome c follows monophasic kinetics. Similar results were obtained when horse heart ferrocyanochrome c was present. The rate constants for the respective reactions are reported in Table XII. It should be noted that ND filters were not used in this section.

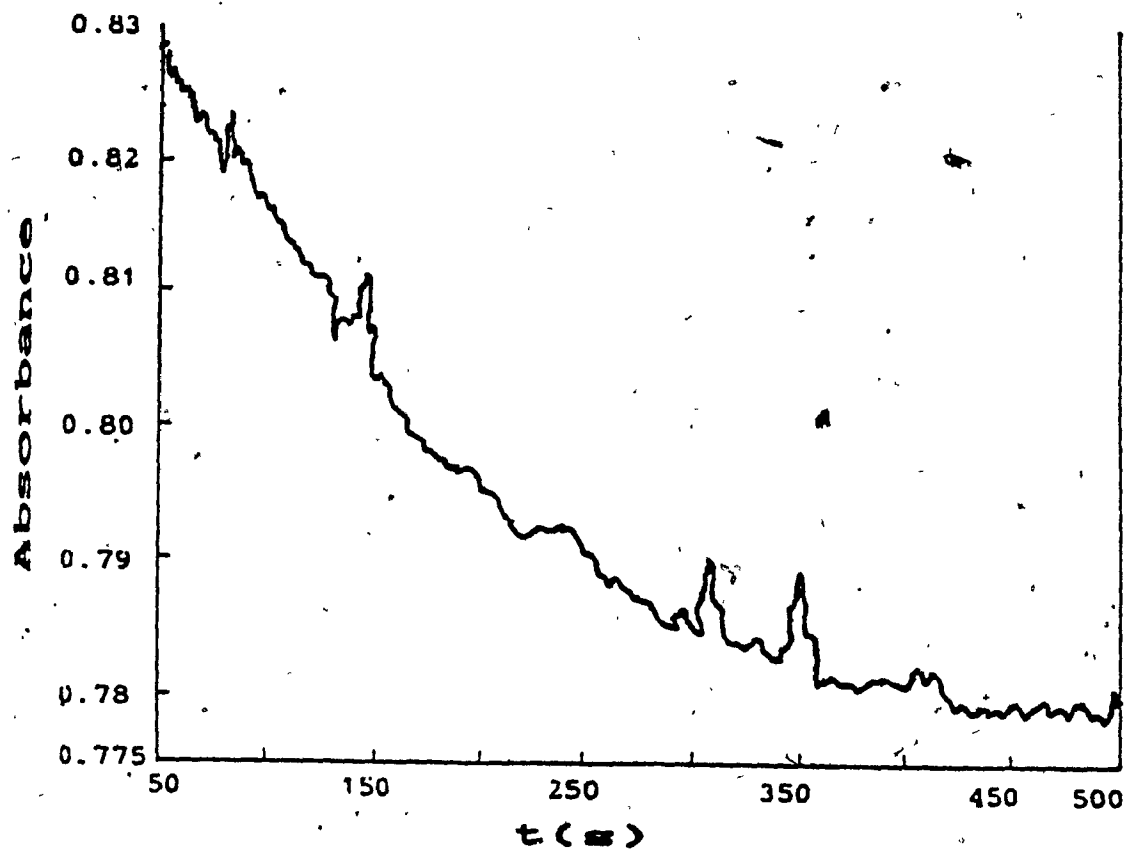


Figure 4.11 Absorbance change at 414 nm due to CCP:CO thermal dissociation in presence of yeast ferrocyclochrome c versus time in 0.01 M phosphate buffer pH 7.0, at $18 \pm 0.5^\circ\text{C}$, under 0.05 atm CO, using NO as trapping agent.

Table XII: Thermal Dissociation Rate Constants for CCP:CO in the Presence and Absence of Ferrocyanochrome c, using NO as a Trap.^a

Ferrocyanochrome	$k^1 \times 10^3$ (s ⁻¹)
horse heart	6.3 ± 0.7
yeast	6.6 ± 0.5
none	5.9 ± 0.7

^a0.01 M phosphate buffer pH 7.0, $18 \pm 0.5^\circ\text{C}$, $P_{\text{CO}} = 0.05$ atm, no ND filter was utilized. $P_{\text{NO}} = 0.1$ atm, $[\text{CCP}] = 2.5 \mu\text{M}$.

4.3 Discussion

4.3.1 Reactions of Horse Heart and Yeast Ferricytochrome c with CCP:CO, at 1 atm CO.

Reactions of horse heart and yeast ferricytochrome c's with the CCP:CO complex were found to be biphasic at 1 atm CO, $18 \pm 0.5^\circ\text{C}$ (Table VII). The slow rate constant for the reaction of horse heart ferricytochrome c was found to show a linear increase with temperature over the range of 6.5 to 32.0°C (Table IX). The activation parameters for this reaction show a distinct difference from those reported for Mb:CO and HRP:CO thermal dissociation (Table X). However, the values found here are similar to those reported for the direct electron transfer between reduced CCP and oxidized cytochrome c (Cheung et al., 1988). The latter study gave the following results: $\Delta H^\ddagger = 4.6 \text{ Kcal mol}^{-1}$, and $\Delta S^\ddagger = -46 \text{ e.u.}$ The results obtained in this study are $\Delta H^\ddagger = 6.4 \text{ kcal mol}^{-1}$ and $\Delta S^\ddagger = -47 \text{ e.u.}$ The discrepancies in the values may be attributed to the difference in the spin state and the coordination of the iron in the two reactions. In unligated CCP^{II} , the iron atom is high spin and five-coordinate as shown from resonance Raman studies (Smulevich et al., 1988), whereas in CCP:CO the iron atom is six-coordinate and low spin. In both reactions the product is CCP^{III} which is five-coordinate, high spin. Thus, oxidation of CCP:CO requires a change in the spin and ligation states of the iron atom which is expected to increase the ΔH^\ddagger for the electron transfer. The slow rate constant is assumed to be the rate of the electron transfer between the horse heart ferricytochrome c and CCP:CO.

It is assumed that the fast rate constant of the reaction of yeast c with CCP:CO is also the electron transfer. Electron transfer between yeast C^{III} and CCP:CO is expected to be more rapid than the electron transfer between horse heart C^{III} and CCP:CO since the rates of the electron transfer between CCP II and C^{III} from horse heart and yeast are 0.23 s^{-1} and 1.7 s^{-1} , respectively (Cheung et al., 1986).⁴ Thus, assigning k^{II} and k^I in Table VII to the reduction rates of yeast C^{III} and horse heart C^{III} , respectively, by CCP:CO is not unreasonable. However, we do not know the nature of the slow phase in Figure 4.6, which like the fast phase for the horse C^{III} reaction with CCP:CO (Figure 4.2), is the minor component.

4.3.2 Reactions of Ferricytochrome c's with CCP:CO at 0.1 and 0.01 atm CO.

The rate for the reaction of horse heart ferricytochrome c was measured at 0.1 and 0.01 atm CO and the magnitude of the rate constant was similar to that reported for the slow phase (major component) at 1 atm CO. Furthermore, the observed trace for the absorbance increase at 414 nm (Figure 4.6) was essentially monophasic.

The yeast ferricytochrome c reaction yielded similar results at 0.1 and 0.01 atm CO. Only the fast or major component observed at 1 atm CO appeared at lower CO pressures. For both cytochromes, the rate constants observed at low CO pressures are similar to those assigned, in the previous section to the electron transfer from CCP:CO to the oxidized cytochrome c.

4.3.3 Thermal Dissociation of CCP:CO in the Presence of Reduced Yeast and Horse Heart Cytochrome c's Using NO as a Trap.

The rate constant reported for CCP:CO dissociation in the presence of reduced yeast and horse heart cytochrome c's (Table XII) are found to be similar to those reported for CCP:CO dissociation in the absence of cytochrome c. These results suggest that the binding of reduced cytochrome c does not have a significant effect upon the CCP:CO dissociation process.

CONCLUSIONS

1. Thermal dissociation rates of CCP:CO and HRP:CO were measured in 0.01 M phosphate buffer, pH 7.0, at $18 \pm 0.5^\circ\text{C}$, using NO and H₂O₂ as trapping agents. The absorbance change was monophasic at 0.1 atm CO and biphasic at 1 atm CO for both peroxidases. These results provide kinetic evidence for the presence of a single CO conformer (Form I) at 0.1 atm CO and the appearance of a new CO conformer (Form II) at 1 atm CO for HRP:CO and CCP:CO, originally reported by Evangelista-Kirkup et al., 1986 and Smulevich et al., 1986, respectively. Only a single rate constant could be measured for alkaline CCP:CO dissociation (pH 8) which is also in agreement with the resonance Raman and infrared data.

2. At high phosphate concentration (0.1 M, pH 8) the fresh CCP:CO dissociation rate constant was ~ 3-fold higher than that for moderately aged CCP:CO. This does not correspond to the results of Smulevich et al., 1986 who reported that the acidic-alkaline transition of the CO conformer was inhibited at high phosphate concentrations.

3. Reactions of horse heart and yeast cytochrome c with CCP:CO complex were also found to be biphasic. The activation parameters for the slow component of the reaction of horse heart C^{III} with CCP:CO: $\Delta H^\ddagger = 6.4 \text{ Kcal mol}^{-1}$ and $\Delta S^\ddagger = -47 \text{ e.u.}$ are similar to those reported for direct electron transfer between CCP^{II} and horse heart C^{III}, (Cheung et al., 1988). Hence, the slow rate constant ($1.3 \times 10^{-3} \text{ s}^{-1}$) is assumed to be the electron transfer rate between horse heart C^{III} and CCP:CO at $18 \pm 0.5^\circ\text{C}$. For the corresponding reaction between yeast C^{III} and CCP:CO at $18 \pm 0.5^\circ\text{C}$, the major electron transfer rate constant is 10

fold faster ($3.0 \times 10^2 \text{ s}^{-1}$). This is in accordance with the direct electron transfer rate measured between CCP^{III} and horse heart and yeast cytochrome c's (Cheung et al., 1986). However, the nature of the minor component in the reactions of cytochrome c with CCP:CO at this stage is not clear and further investigations are necessary to clear this part of the study. At low CO concentrations only a single electron transfer rate was observed between respective ferricytochrome c's and CCP:CO which is similar to the magnitude of the major electron transfer rate constant at 1 atm CO.

4. Measurements of CCP:CO dissociation in the presence and absence of reduced horse heart and yeast cytochrome c's, using NO as trapping agent indicate that the binding of the reduced cytochrome c does not affect the CCP:CO dissociation rate.

SUGGESTIONS FOR FURTHER EXPERIMENTS

1. NO is known to bind to ferroperoxidases (Mims et al., 1983; Yonetani et al., 1972) as well as to ferriperoxidases (Tamura et al., 1978). As discussed previously cytochrome c binds to peroxidases in solution at various ionic strengths (Cheung and English, 1988). Therefore, cytochrome c is expected to also bind to $\text{CCP}^{\text{II}}:\text{NO}$ and to $\text{CCP}^{\text{III}}:\text{NO}$ in solution. Mochan and Nicholls (1971) found that the rate of H_2O_2 reaction with CCP remained unaffected in the presence of cytochrome c. Therefore, it is reasonable to assume that the presence of cytochrome c would not interfere with NO ligation to CCP^{II} . If our predictions about the NO ligation to the peroxidases, in the presence of cytochrome, mentioned above are true, then it would be beneficial to determine the activation parameters of the reaction of ferricytochrome c with $\text{CCP}^{\text{II}}:\text{NO}$ in 0.01 M phosphate buffer, pH 7.0. Since NO reacts with both reduced and oxidized form of cytochrome c peroxidase, it may be possible to measure ΔH^\ddagger and ΔS^\ddagger of the intramolecular electron transfer in $\text{C}^{\text{III}}/\text{CCP}^{\text{II}}:\text{NO}$. Under these circumstances, the spin state and the coordinate number of the iron in CCP may remain constant, because NO does not dissociate from CCP in any redox state. Comparison of ΔH^\ddagger and ΔS^\ddagger of this reaction with those reported in Chapter 4 (for $\text{C}^{\text{III}}/\text{CCP}^{\text{II}}:\text{CO}$), may reveal the influence of the change of spin state and of the coordination number of the iron upon the magnitude of intramolecular electron transfer reaction in $\text{C}^{\text{III}}/\text{CCP}^{\text{II}}$. It should be noted that NO is known to bind to horse heart C^{III} in solution (Kon, 1969). However C^{III} (horse heart) has lower affinity for NO than

CCP^{III}. Therefore it is recommended to measure the intramolecular electron transfer in C^{III}/CCP^{III}:NO at very low NO concentrations ($\leq 1 \mu\text{M}$). Under these conditions NO binding to horse C^{III} may be negligible and NO may remain bound to CCP^{III}.

2. Comparison of CCP:CO and HRP:CO thermal dissociation rate constants at 0.1 and 0.01 atm CO, in the presence and absence of ND filters (Tables III and IV), suggested that there may be some error introduced in the magnitude of k^{\ddagger} due to some photoassisted dissociation. In Chapter 4, the activation parameters of the slow component of the reaction of horse heart C^{III} with CCP:CO were reported in the absence of ND filters. Therefore photoassisted dissociation might have also introduced some error in the magnitude of the activation parameters. In order to determine the exact values of ΔH^{\ddagger} and ΔS^{\ddagger} , it is recommended to study the reaction of horse heart C^{III} with CCP:CO in the presence of a 13% transmittance ND filter.

REFERENCES

Antonioni, E., Brunori, M., Hemoglobin and Myoglobin in Their Reactions with Ligands, North Holland Publishing Company, Vo. 21 (1971).

Baldwin, J.M., J. Mol. Biol., 136, 103 (1980).

Bonaventura, C., Bonaventura, T., Antonioni, E., Brunori, M., Wyman, Y., Biochemistry, 12, 3424 (1973).

Brozowski, A., Derewenda, A., Dodson, E., Dodson, G., Grabowski, M., Liddington, R., Scharzyski, T., and Valley, D., Nature, 307, 74 (1984).

Brauman, J.I., Rose, E., and Suslick, K.S., J. Amer. Chem. Soc., 102, 3224 (1980).

Brudvig, G.W., Stevens, T.H., and Chan, S.I., Biochemistry, 19 (1980).

Brunori, M., Bonaventura, T., Bonaventura, C., Antonioni, E., and Wyman, T., Proc. Natl. Acad. Sci. U.S.A., 69, 868 (1972).

Case, D.A., Karplus, M.J., J. Mol. Biol., 132, 343 (1979).

Caughey, W.S., Ann. N.Y. Acad. Sci., 174, 148 (1970).

Chance, B., Arch. Biochem. Biophys. 41, 404 (1952).

Chang, C.K., Traylor, T.B., Proc. Natl. Acad. Sci., U.S.A., 72, 1166 (1975).

Cheung, E., Taylor, K., Kornblatt, J.A., English, A.M., McLendon, G., and Miller, Y.R. Proc. Natl. Acad. Sci., U.S.A. 83, 1330 (1986).

Cheung, E. and English, A.M., Inorg. Chem., 27, 1078 (1988).

Coletta, M., Ascoli, F., Brunori, M., and Traylor, T.G., J. Biol. Chem., 261, 9811 (1986).

Collman, J.P., Brauman, Y.I., Halbert, T.R., Suslick, K.S., Proc. Natl. Acad. Sci., U.S.A., 73, 3333 (1976).

Dickerson, R.E., and Geis, I., in Hemoglobin : Structure, Function, Evolution, and Pathology, Benjamin/Cummings Publishing, Menlo Park, CA (1983).

Dowé, R.T., Vitello, L.B., J. Biol. Chem. 255, 6224 (1980).

Edwards, S.L., Poulos, P.L., and Kraut, J., Biol. Chem., 259, 1284 (1984).

English, A.M., Laberge, M., and Walsh, M., *Inorg. Chim. Acta*, 123, 113 (1986).

English, A.M., McLendon, G., and Taylor, K., *J. Amer. Chem. Soc.*; 106, 644 (1984).

Erman, J.E., and Vitello, L.B., *J. Biol. Chem.*, 255, 6224 (1980).

Evangelista-Kirkup, R., Smulevich, G., Spiro, T.G., *Biochemistry*, 25, 4420 (1986).

Fermi, G., *J. Mol. Biol.*, 97, 237 (1975).

Finzel, B.C., Poulos, T.L. and Kraut, J., *J. Biol. Chem.*, 259, 13027 (1984).

Gibel, Y., Cannon, Y., Campbell, D., and Traylor, T.G., *J. Amer. Chem. Soc.*, 100, 3575 (1978).

George, P., *J. Biol. Chem.* 201, 427 (1953).

Gupta, R.K., and Yonetani, T., *Biochim. Biophys. Acta.*, 292, 502 (1973).

Hayashi, Y., Yamada, H., and Yamazaki, I., *Biochim. Biophys. Acta*, 427, 608 (1976).

Hazzard, J.T., Poulos, T.L., Tollin, G., *Biochemistry*, 26, 2836 (1987).

Ho, P.S., Sutoris, C., Liang, N., Margoliash, E. and Hoffman, B.M., *J. Amer. Chem. Soc.*, 107, 1070 (1985).

Hoth, L.R. and Erman, J.E., *Biochim. Biophys. Acta*, 788, 151 (1984).

Hoshimoto, T., Dyer, R.L., Crossley, M.J., Baldwin, Y.E. and Bassolo, F., *J. Amer. Chem. Soc.*, 104, 2101 (1982).

Jameson, G.B., Molinaro, F.S., Ibers, J.A., Collman, J.P., Brauman, J.I., Rose, E., and Suslick, K.S., *J. Amer. Chem. Soc.*, 102, 3224 (1980).

Iizuka, T., Makino, R., Ishimura, Y., Yonetani, T., *J. Biol. Chem.*, 260, 1407 (1985).

Kang, C.H., Ferguson-Miller, S., and Margoliash, E., *J. Biol. Chem.*, 252, 919 (1977).

Kang, D.S., and Erman, E.E., *J. Biol. Chem.*, 257, 12775 (1982).

Keilin, D., and Hartree, E.F., *Biochem. J.*, 61, 153 (1955).

- Kertesz, D., Antonioni, E., Brunori, M., Wyman, J. and Zito, R., *Biochemistry*, 4, 2672 (1965).
- Kon, H., *Biochem. Biophys. Res. Commun.*, 35, 423 (1969).
- Koppenol., W.H. and Margoliash, E., *J. Biol. Chem.*, 2757, 4426 (1982).
- Kornblatt, J.A. and English, A.M., *Eur. J. Biochem*, 155, 505 (1986).
- Leonard, J.J., and Yonetani, T., *Biochemistry*, 13, 1465 (1974).
- Loo, S. and Erman, J.E., *Biochemistry*, 14, 3467 (1975).
- Margoliash, E., and Prohwirt, M., *J. Biochem.*, 71, 571 (1959).
- Mathews, R.A. and Wittenberg, J.B., *J. Biol. Chem.*, 254, 5991 (1979).
- Mims, M.P., Porras, A.G., Olson, J.S., Noble, R.W., Peterson, J.A., *J. Biol. Chem.*, 258, 14219 (1983).
- Mochan, E., *Biochim. Biophys. Acta*, 216, 80 (1970).
- Mochan, E., and Nicholls, P., *Biochem. J.* 121, 69 (1971).
- Momenteau, N., and Lavalette, D., *J. Chem. Soc. Chem. Comm.*, 341 (1982).
- Nelson, C.E., Sitzman, E.Y., Kang, C.H., and Margoliash, E., *Anal. Biochem.*, 83, 622 (1977).
- Ng Ching Hing, K.C., B.Sc. Thesis, Concordia University (1985).
- Ohlsson, P.I. and Paul, K.G., *Acta. Chem. Scand. B* 30, 373 (1976).
- Phelps, C., Antonioni, E., and Brunori, M., Wyman, J., and Zito, R., *Biochem. J.*, 122, 79 (1971).
- Phillips, S.E.Y., and Schoenborn, B.P., *Nature*, 292, 81 (1981).
- Poulos, T.L. and Kraut, J., *Biol. Chem.*, 255, 10322 (1980).
- Poulos, T.L. and Finzel, B.C., *Heme Structure and Function*, *Pept. Prot. Rev.*, 4 (1984).
- Poulos, T.L., Freer, S.T., Alden, R.A., Xuong, Ng. H., Edwards, S.L., Hamlin, R.C., and Kraut, J., *J. Biol. Chem.*, 253, 3730 (1978).
- Satterlee, J.D., and Erman, J.E., *J. Amer. Chem. Soc.*, 106, 1140 (1984).
- Sawicki, C.A., Gibson, Q.H., *J. Biol. Chem.*, 251, 1533, (1976).

Sawicki, C.A., and Gibson, Q.H., J. Biol. Chem., 252, 7538 (1977).

Shaanan, B., Nature, 296, 683 (1982).

Smith, M.L., Ohlsson, P.I., Paul, K.G., FEBS Lett., 163, 303 (1983).

Smulevich, T., Evangelista-Kirkup, R., English, A., and Spiro, T.G., Biochemistry, 25 (1986).

Smulevich, G., Dasgupta, S., English, A., and Spiro, T.G., Biochim. Biophys. Acta, 873, 88 (1986).

Smulevich, G., Mauro, M.J., Fishel, L.A., English, A.M., Kraut, J., and Spiro, T.G., Biochemistry, (1988) in Press.

Suslick, K.S., Fox, M.M., Reinert, T.Y., J. Amer. Chem. Soc., 106, 4522 (1984).

Suslick, K.S., and Reinert, T.J., J. Chem. Ed., 62, 974 (1985).

Swinbourne, E.S., Analysis of Kinetic Data, Nelson (1971).

Takano, T., J. Mol. Biol., 110, 569 (1977).

Tamura, M., Kobayashi, K., and Hayashi, K., FEBS Letters, 88, 124 (1978).

Traylor, T.G., Berzinius, A.P., Proc. Natl. Acad. Sci., U.S.A. 77, 3171 (1980).

Traylor, T.G., Mitchell, M.J., Tsuchiya, S., Campbell, D.H., Stykes, D., and Koga, N.Y., J. Amer. Chem. Soc., 103, 5234 (1981).

Traylor, T.G., Tsuchiya, S., Campbell, D., Mitchell, M., Stykes, D., and Koga, N., J. Amer. Chem. Soc., 107, 604 (1985).

Ward, B., Wang, C.B., Chang, C.K., J. Amer. Chem. Soc., 103, 5236 (1981).

Ward, B., and Chang, C.K., Photochem. Photobiol., 35, 757 (1982).

Weast, R.C. (ed.), Handbook of Chemistry and Physics CRC Press Inc., B-102 (1980-81).

Wittenberg, B.A., Brunori, M., Antonioni, E., Wittenberg, J.B., and Wyman, J. Arch. Biochem. Biophys., 111, 576 (1965).

Wittenberg, B.A., Antonioni, E., Brunori, M., Noble, R.W., Wittenberg, J.B., and Wyman, T., Biochemistry, 6, 1970 (1967).

Yonetani, T., The Enzymes, (Boyer, P.D., ed.), 13, 345, Academic Press, FL (1976).

Yonetani, T., J. Biol. Chem. 240, 4509 (1965).

Yonetani, T., Yamamoto, H., Erman, J.E., Leigh, J.S., and Reed, G.H., J. Biol. Chem. 247, 2447 (1972).

Yonetani, T. and Anni, H., J. Biol. Chem., 262, 1 (1987).

Young, R., Chang, C.K., J. Amer. Chem. Soc., 107, 898 (1985).

Yu, N.T., Kerr, E.A., Ward, B. and Chang, C.K., J. Amer. Chem. Soc., 22, 4534 (1983).